Matthew J. Budoff
Stephan S. Achenbach
Harvey S. Hecht
Jagat Narula
Editors

Atlas of Cardiovascular Computed Tomography

Second Edition

Springer

Atlas of Cardiovascular Computed Tomography

Matthew J. Budoff • Stephan S. Achenbach
Harvey S. Hecht • Jagat Narula
Editors

Atlas of Cardiovascular Computed Tomography

Second Edition

Springer

Editors
Matthew J. Budoff
Los Angeles Biomedical Research Institute
UCLA
Torrance, California, USA

Stephan S. Achenbach
Department of Cardiology
Universitätsklinikum Erlangen
Erlangen, Germany

Harvey S. Hecht
Mount Sinai Hospital
New York City, New York, USA

Jagat Narula
Department of Cardiology
Mount Sinai Hospital
New York City, New York, USA

Previously published by Springer, New York (2007) 978-1-57340-267-5
ISBN 978-1-4471-7356-4 ISBN 978-1-4471-7357-1 (eBook)
https://doi.org/10.1007/978-1-4471-7357-1

Library of Congress Control Number: 2017964096

Printed on acid-free paper

This Springer imprint is published by the registered company Springer-Verlag London Ltd. part of Springer Nature.
The registered company address is: The Campus, 4 Crinan Street, London, N1 9XW, United Kingdom

Preface

Over the past decade, the technology of cardiovascular CT and its clinical utility have grown enormously. Appropriateness use criteria and credentialing standards are being developed at a record pace.

Physicians currently training in cardiology and radiology undergo mandatory training in cardiac CT, and the American College of Cardiology, American Heart Association, Society of Cardiovascular Computed Tomography and American College of Radiology have published scientific statements and guidelines to support the use of this diagnostic modality in clinical practice. Although this rapid evolution of knowledge and experience has been accompanied by a large number of scientific publications, there has been a relative lack of high-quality, practical, and comprehensive training material. In an area based on imaging, a comprehensive atlas should form a central piece of information and reference. We have assembled the foremost authorities in the field to author chapters for this Atlas of Cardiovascular Computed Tomography. The images within will provide the cardiac CT enthusiast with a didactically useful introduction to the field yet sufficiently comprehensive to provide the advanced user with excellent examples of common and uncommon CT findings.

The evolution of cardiovascular CT imaging has been accompanied by significant controversy regarding its clinical applicability. However, the breathtakingly rapid improvement in CT imaging technology, especially since the introduction of advanced multidetector CT systems, has vaulted CT imaging into mainstream cardiology practice, and there is uniform consensus that its utility will continue to expand in the coming years. Imaging with multidetector CT allows assessment of coronary artery stenoses with stunning spatial and temporal resolution. Beyond the mere detection of flow-limiting stenoses in coronary artery disease, great strides have been made in the identification of plaque characteristics that confer higher risk. The diagnosis of coronary artery disease has evolved from the assessment of disease sequelae to the early detection of the pathologic process itself, before the consequences become clinically manifest through ischemic symptoms, myocardial infarction, or sudden death. As presented in the following chapters, cardiac CT has matured significantly and become a valid risk-stratifying tool for the early detection of atherosclerosis through coronary artery calcium scanning, a possible replacement for noninvasive exercise testing as the test of choice for the evaluation of chest pain in stable patients, and a powerful tool to image for congenital heart disease, venoatrial anatomy before electrophysiologic testing, and peripheral artery disease. The atlas focuses on the pearls and pitfalls of cardiovascular CT and not only offers excellent images but also discusses problems encountered during CT imaging and suboptimal results.

We are confident that this atlas offers an exceptional compilation of information and comprehensively reflects the current state of the art in cardiovascular CT. We believe that you will find this atlas as enjoyable as it is educational.

Torrance, CA, USA — Matthew J. Budoff
Erlangen, Germany — Stephan S. Achenbach
New York, NY, USA — Harvey S. Hecht
New York, NY, USA — Jagat Narula

Contents

1 **Historical Perspective** 1
Stephan S. Achenbach

2 **Preparation, Image Acquisition and Reconstruction, and Post-processing** 13
Jamaluddin Moloo, Udo Hoffmann, and Harvey S. Hecht

3 **Normal Coronary Anatomy** 35
Farhood Saremi, Stephan S. Achenbach, and Jagat Narula

4 **Coronary Artery Calcium in Primary Prevention** 49
Harvey S. Hecht and Matthew J. Budoff

5 **Assessment of Native Coronary Artery Disease** 69
Stephan S. Achenbach

6 **Imaging of High-Risk Atherosclerotic Plaques** 101
Amir Ahmadi, Kenichi Sakakura, Kazuyuki Yahagi, Renu Virmani, and Jagat Narula

7 **Coronary Stents: Evaluation and Follow-up** 121
Harvey S. Hecht, Annapoorna Kini, and Samin Sharma

8 **Cardiac CT Before and After Bypass Graft Surgery** 145
Koen Nieman

9 **Functional Significance of Coronary Stenoses Identified by CT** 165
Joshua Schulman-Marcus and James K. Min

10 **Cardiac CT in the Emergency Department** 177
Maros Ferencik, Khristine Ghemigian, and Udo Hoffmann

11 **Imaging Diseases of the Aorta** 191
Peter S. Fail

12 **Imaging of the Peripheral Vasculature and Carotid Arteries** 205
Peter S. Fail and Vinod Nair

13 **Valvular Diseases and Interventions** 221
Philipp Blanke, Angus Thompson, and Jonathon Leipsic

14 **CT in the Management of Cardiac Arrhythmias** 271
Joel Wilson, Farhood Saremi, Jagat Narula, and Sanjiv M. Narayan

15 **Myocardial Function and Viability** 303
Andreas H. Mahnken

16 **Coronary Artery Anomalies** 325
Edward D. Nicol and Simon P.G. Padley

17 Congenital Heart Disease 339
Priya Pillutla and Jamil A. Aboulhosn

18 Devices and Implants 351
Christopher M. Walker, Quynh A. Truong, and Suhny Abbara

19 Appropriateness Use Criteria and Guidelines for CT Use 381
Joshua Schulman-Marcus and James K. Min

Index 389

Contributors

Suhny Abbara Department of Radiology, Division of Cardiothoracic Imaging, UT Southwestern Medical Center, Dallas, TX, USA

Jamil A. Aboulhosn Ronald Reagan/UCLA Medical Center, Ahmanson Adult Congenital Heart Disease Center, Los Angeles, CA, USA

Stephan S. Achenbach Department of Cardiology, University of Erlangen, Erlangen, Germany

Amir Ahmadi Department of Cardiology, Icahn School of Medicine at Mount Sinai, New York, NY, USA

Philipp Blanke Department of Radiology, Centre for Heart Valve Innovation, St Paul's Hospital, Vancouver, BC, Canada

Matthew J. Budoff UCLA Los Angeles Biomedical Research Institute, Torrance, CA, USA

Peter S. Fail Department of Interventional Cardiology, Cardiovascular Institute of the South/ Terrebonne General Medical Center, Houma, LA, USA

Maros Ferencik Knight Cardiovascular Institute, Oregon Health and Science University, Portland, OR, USA

Khristine Ghemigian Department of Radiology, Massachusetts General Hospital and Harvard Medical School, Boston, MA, USA

Harvey S. Hecht Department of Cardiology, Icahn School of Medicine at Mount Sinai, New York, NY, USA

Udo Hoffmann Department of Radiology, Massachusetts General Hospital, Boston, MA, USA

Annapoorna Kini Department of Cardiology, Icahn School of Medicine at Mount Sinai, New York, NY, USA

Jonathon Leipsic Department of Radiology, St. Paul's Hospital, Vancouver, BC, Canada

Andreas H. Mahnken Department of Diagnostic and Interventional Radiology, Marburg University Hospital, Marburg, Germany

James K. Min Dalio Institute of Cardiovascular Imaging, New York-Presbyterian Hospital and Weill Cornell Medicine, New York, NY, USA

Jamaluddin Moloo Cardiac Vascular Center, University of Colorado, Denver, CO, USA

Vinod Nair Cardiovascular Institute of the South, Houma, LA, USA

Sanjiv M. Narayan Department of Medicine/Division of Cardiology, Stanford University, Stanford, CA, USA

Jagat Narula Mount Sinai Heart, Icahn School of Medicine at Mount Sinai, New York, NY, USA

Edward D. Nicol Department of Cardiac CT, Royal Brompton Hospital, London, UK

Koen Nieman Stanford University School of Medicine, Stanford, CA, USA

Simon P.G. Padley Department of Cardiac CT, Royal Brompton Hospital, London, UK

Priya Pillutla Division of Cardiology, Department of Medicine, Los Angeles Medical Center, Harbor-University of California, Torrance, CA, USA

Kenichi Sakakura CVPath Institute Inc., Gaithersburg, MD, USA

Farhood Saremi Department of Radiology, University of Southern California, USC University Hospital, Los Angeles, CA, USA

Joshua Schulman-Marcus Department of Cardiology, Albany Medical Center, Albany, NY, USA

Samin Sharma Cardiovascular Institute, Icahn School of Medicine at Mount Sinai, New York, NY, USA

Angus Thompson Department of Radiology, St Paul's Hospital, University of British Columbia, Vancouver, BC, Canada

Quynh A. Truong Department of Radiology, Weill Cornell Medical Center, New York, NY, USA

Renu Virmani CVPath Institute Inc., Gaithersburg, MD, USA

Christopher M. Walker Department of Radiology, Saint Luke's Hospital of Kansas City, Kansas City, MO, USA

Joel Wilson Division of Cardiovascular Medicine, UCSD Medical Center, La Jolla, CA, USA

Kazuyuki Yahagi CVPath Institute Inc., Gaithersburg, MD, USA

Historical Perspective

1

Stephan S. Achenbach

On November 8, 1895, Wilhelm Conrad Röntgen (1845–1923) discovered X-rays in his laboratory at the University of Würzburg, Germany. In 1901, he was awarded the first Nobel Prize in Physics "*in recognition of the extraordinary services he has rendered by the discovery of the remarkable rays subsequently named after him.*" Röntgen declined to patent his discovery, so that it could be more widely used. Consequently, imaging with X-rays was rapidly introduced into medical diagnostics.

The diagnostic capabilities of X-ray imaging were dramatically increased when computed tomography (CT) was developed in the late 1960s. X-ray CT became possible because of the advent of digital data processing through computers and the availability of mathematical methods to generate cross-sectional images based on numerous X-ray projections obtained from various orientations. The required mathematical methods had been pioneered by scientists such as the Norwegian Niels Henrik Abel (1802–1829), the Austrian Johann Radon (1887–1956), and the South African physicist Allen McLeod Cormack (1924–1988), who, in fact, built a prototype tomographic device in 1963 but was not interested in any practical applications [1]. Independently, the British engineer Sir Godfrey Newbold Hounsfield (1919–2004) conceived the concept of computed tomography X-ray imaging in the late 1960s while he was working as an inventor for a company called "Electrical and Musical Industries" (EMI) and was generously funded by income EMI generated through the tremendous commercial success that the Beatles enjoyed under their cover [2]. Allegedly, Hounsfield developed the basic idea during an outing in the country. Unaware of previous work, he solved the underlying mathematical problem and constructed a prototype CT scanner in 1967, originally using a source of gamma radiation, then to be replaced by an X-ray tube. Initial acquisitions on preserved human brains took 9 days for a single cross-sectional image. The invention was patented in 1968. On October 1, 1971, X-ray CT was introduced into medical practice when a first patient with a cerebral cyst underwent a brain scan at Atkinson Morley Hospital in Wimbledon, London, United Kingdom. The scan time was 4.5 min to generate an image 13 mm thick with a resolution of 80 × 80 pixels. Technical progress rapidly improved both acquisition protocols and image quality. CT scanners, initially with scan times of about 20 s per image, became commercially available through numerous companies from 1973 on. In 1979, Cormack and Hounsfield jointly received the Nobel Prize in Physiology or Medicine.

This chapter is dedicated to the memory of David G. King (1947–2004), an assistant to Sir Godfrey Hounsfield in his early career and a tireless supporter of research in cardiac CT, often referred to as the "father of coronary calcium scanning."

S.S. Achenbach
Department of Cardiology, University of Erlangen,
Erlangen, Germany
e-mail: stephan.achenbach@uk-erlangen.de

M.J. Budoff et al. (eds.), *Atlas of Cardiovascular Computed Tomography*, https://doi.org/10.1007/978-1-4471-7357-1_1

Approaches to Cardiac Computed Tomography

The principle of computed tomography (CT) is to obtain a cross-sectional image based on X-ray acquisitions obtained from various orientations in a single slice of the body. Roughly speaking, at least 180° of projections are required (as acquisitions from exactly opposite directions would yield identical attenuation data). CT systems that required mechanical motion of an X-ray source around the body had scan times of approximately 3 s per slice into the 1980s. Even after the introduction of slip-ring technology, which allowed continuous rotation of the gantry, and "helical" or "spiral" acquisition, which combined continuous gantry rotation with continuous table motion in 1989 by Willi Kalender [3], image acquisition times remained in the 1-s range, which was too slow for imaging of the rapidly moving heart. All the same, interest in extending the advantages of tomographic imaging to the heart led to specific developments that were designed to maximize the temporal resolution of CT and allow synchronization to the heartbeat through the patient's ECG, so that cardiac imaging would become possible.

One approach developed in the early 1980s was the Dynamic Spatial Reconstructor, which consisted of 28 X-ray tubes that rotated around the patient at 50 rotations per minute; the images were amplified by 28 TV cameras mounted behind a curved fluorescent screen (58-cm radius) opposite the tubes. Temporal resolution was 16 ms per cross-sectional image and cardiac imaging was possible, but because of its immense size and weight (15 tons), the system was not practical for clinical use and only one such device was ever installed (at the Mayo Clinic in Rochester, MN) [4].

A second approach was the "electron beam computed tomography" (EBCT) system introduced in the late 1980s [5]. Instead of an X-ray tube, which must rotate mechanically around the patient, it used an electron beam, which was deflected by electromagnetic coils to sweep across semicircular targets arranged around the patient. Where the electron beam hit the targets, X-rays were created. The radiation passed through the patient and attenuation was recorded by stationary detectors arranged on the opposite side. Temporal resolution was high at 100 ms, but slice thickness was limited to 1.5 or 3.0 mm, image noise was relatively high, and the cost was substantially more than conventional, mechanical CT systems. The EBCT system was initially designed to study myocardial perfusion and cardiac function, but it was not extensively used for this purpose. Instead, pioneers of cardiac CT such as Arthur Agatston and Warren Janowitz demonstrated the utility of CT imaging for coronary calcium assessment in 1989 and subsequent years [6]. Following were the first contrast-enhanced acquisitions to visualize the coronary artery lumen in 1994 and the first reports that coronary artery stenoses could be detected [7–9]. Ultimately, the image quality that could be obtained by EBCT was not sufficient for clinical applications, but its success in visualizing the coronary arteries and the early demonstration of clinical applications for risk stratification and stenosis detection sparked tremendous interest in further developing mechanical CT, with the aim of providing high-resolution imaging of the heart and coronary arteries [10]. This third approach to cardiac CT imaging, which became available around the year 2000, required several developments: First, CT systems with gantry rotation times of 0.5 s or less were combined with ECG-synchronized image reconstruction methods that used only parts of the rotation, so that high temporal resolution could be achieved. Second, strong X-ray tubes provided sufficient output to keep image noise low despite thin-slice acquisition and short acquisition times. Finally, the acquisition of several slices simultaneously allowed the creation of thin images while keeping overall acquisition time short enough to complete an examination with one breathhold. The first systems acquired four slices simultaneously, so that approximately 35–40 s were required to obtain one data set of the heart with a slice thickness of 1.0 mm [10]. Manufacturers rapidly introduced systems with faster rotation and the ability to acquire more and thinner slices. For example, 16-slice CT with 375 ms rotation time was introduced in 2004, and 64-slice CT systems with rotation times of 330 ms became available around 2005. Currently, high-end systems provide rotation times of about 300 ms, and the widest detectors have 320 rows. At a collimated slice thickness of 0.5 mm, a scan volume of 16 cm can be covered, which is sufficient to cover the heart in one single partial rotation.

A further significant direction of development was dual-source CT, first introduced in 2006 [11]. It combines two X-ray tubes and two detectors arranged at an angle of approximately 90°. Hence, dual-source CT permits the collection of the required data in 180° of projections during a quarter rotation of the X-ray gantry, whereas single-source CT requires a half rotation. Dual-source CT therefore improves temporal resolution by a factor of two. With a gantry rotation time of 0.28 s for the latest dual-source CT system, the temporal resolution of each acquired slice is 75 ms. (It does not exactly correspond to a one-quarter rotation time because the two tubes and detectors are not aligned exactly at a 90° angle.)

Overall, numerous hardware advancements have had substantial influence on image quality in cardiac CT, far beyond the rotation time and number of acquired slices. Over the years, CT imaging—which was initially almost entirely focused on visualization of the coronary arteries—has been able to substantially increase robustness, image quality, and clinical applicability for coronary artery visualization (Figs. 1.1, 1.2, 1.3, 1.4, 1.5, 1.6, 1.7, 1.8, and 1.9).

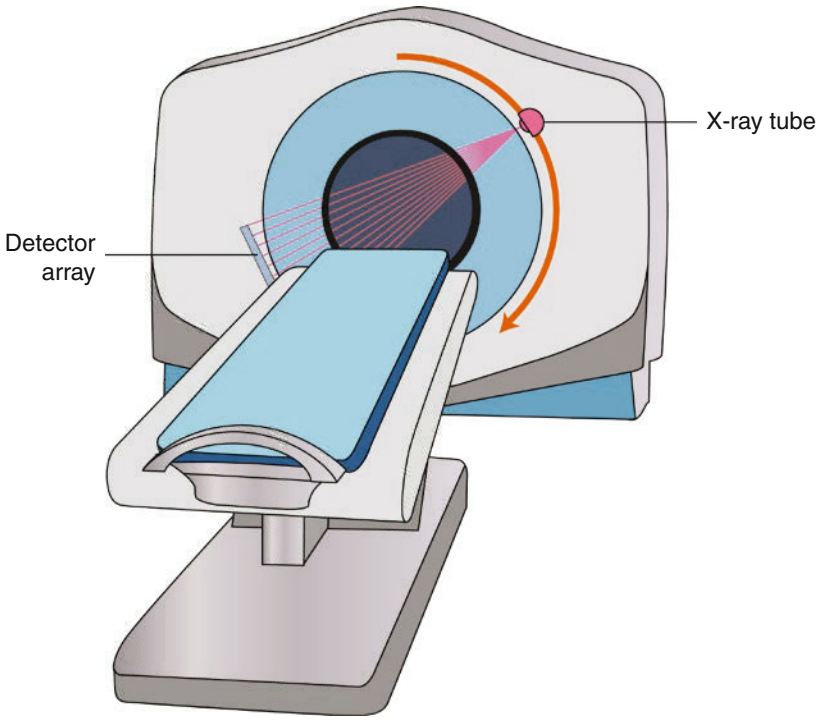

Fig. 1.1 Principle of computed tomography (CT) for imaging. X-ray attenuation data must be acquired from a multitude of projections (at least 180° plus the width of the fan angle of the X-ray beam). This aim is typically achieved by rotating around the patient a gantry that contains an X-ray tube on one side and a detector array on the opposite side. The rotation speed determines the temporal resolution of the acquired image. Systems with multiple detector rows permit the acquisition of more than one cross-sectional image during one rotation

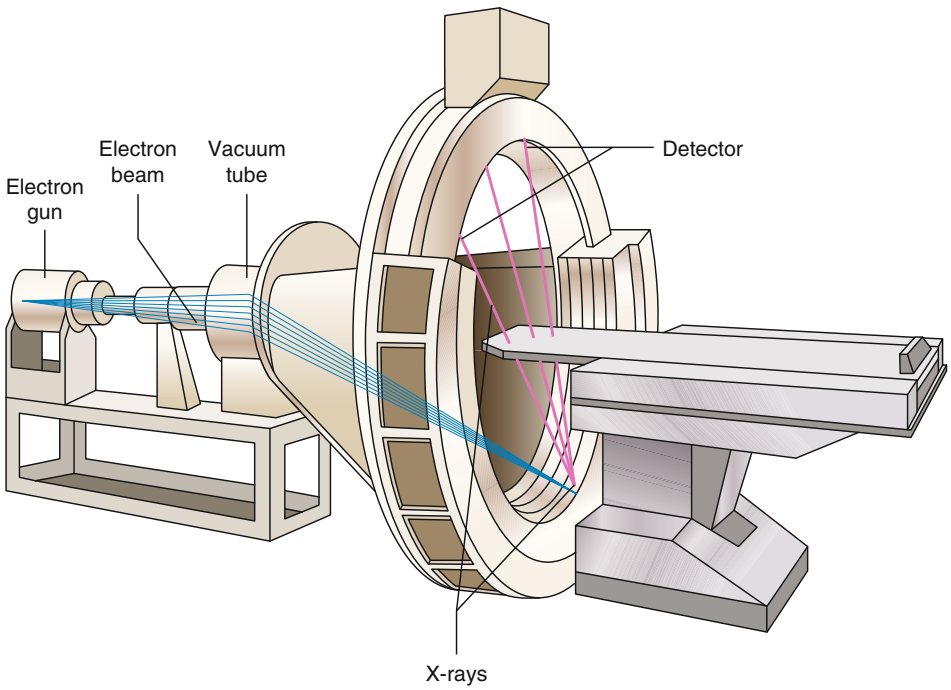

Fig. 1.2 Electron beam CT. The electron beam CT (EBCT) scanner was designed to provide sufficient temporal resolution for cardiac imaging. To avoid rotation of an X-ray tube, an electron beam was created by an electron gun inside a very large vacuum tube. The electron beam was focused and deflected by electronic coils to rapidly sweep across stationary, semicircular targets that were arranged below and around the patient. Where the electron beam hit the targets, X-rays were created. The collimated X-rays penetrated the patient, and attenuation was recorded by stationary detectors. Temporal resolution was 100 ms, with the ability to trigger image acquisition by the patient's ECG. Stepwise motion of the patient table would allow acquisition of a set of approximately 40 slices of 3.0 mm slice thickness to cover the volume of the heart

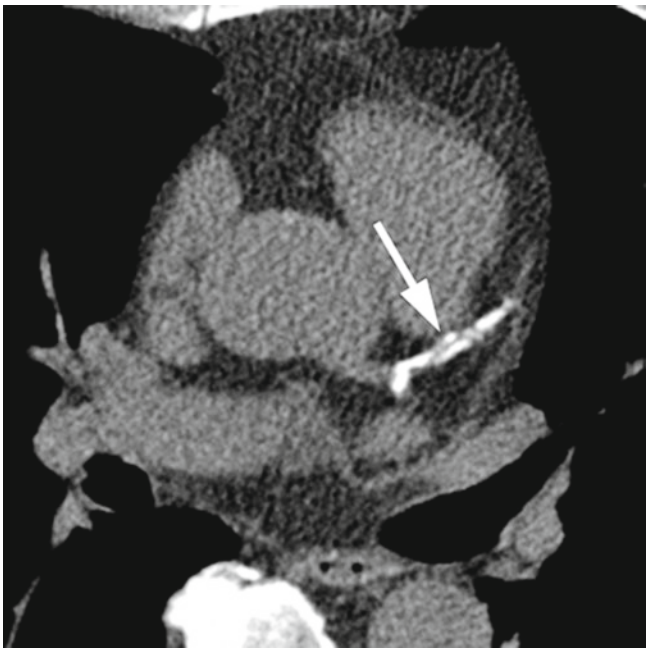

Fig. 1.3 Detection of coronary calcium by EBCT. The first clinical application of cardiac CT was the detection and quantification of coronary calcium for the purpose of risk stratification. Here, a cross-sectional EBCT image (3.0 mm slice thickness, 100 ms acquisition time) shows calcification of the left main bifurcation, proximal left circumflex, and proximal left anterior descending coronary artery (*arrow*)

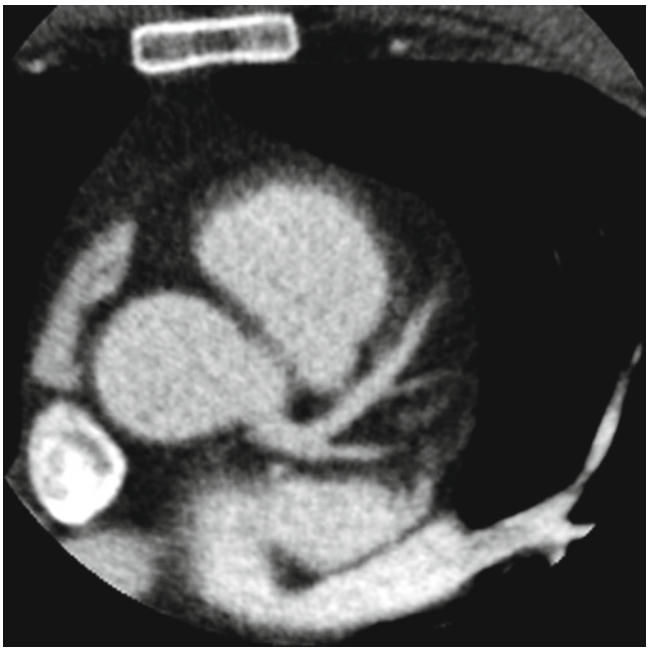

Fig. 1.4 Coronary CT angiography by EBCT. This contrast-enhanced transaxial image shows the proximal left main, left anterior descending, and left circumflex coronary arteries (3.0 mm slice thickness, 100 ms acquisition time)

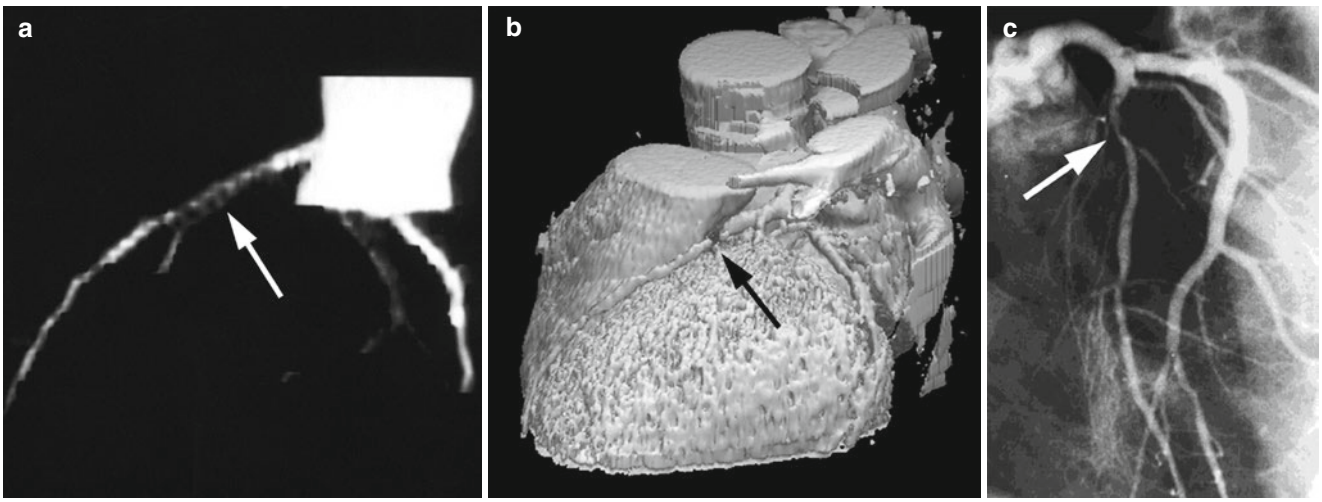

Fig. 1.5 Detection of coronary artery stenoses by EBCT. Multiplanar reconstruction (**a**) and three-dimensional reconstruction (**b**) of the left anterior descending coronary artery show a high-grade stenosis (*arrow*). The invasive coronary angiogram (**c**) confirms the presence of a high-grade stenosis. Though the 3D reconstruction conveys a smooth image impression, the multiplanar reconstruction reveals the relatively crude image quality of EBCT. With 3.0 mm slice thickness per acquired axial image and the need for a breathhold of approximately 40 s, EBCT was not clinically robust enough to reliably detect and rule out coronary artery stenoses

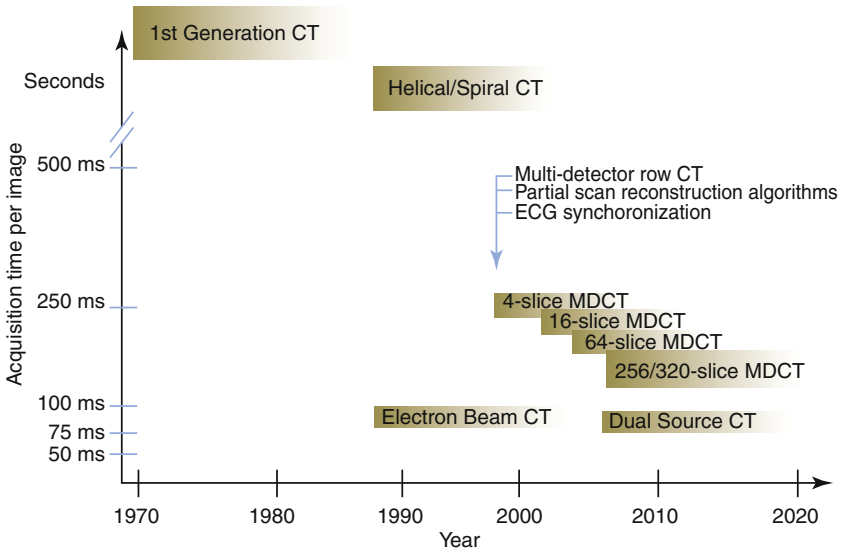

Fig. 1.6 Evolution of technology for cardiac CT. This schematic representation (approximate and not to scale) illustrates the various generations of CT technology in relation to the time of first availability and approximate temporal resolution (time to acquire one cross-sectional image). Note that beyond the acquisition time and number of acquired slices, numerous other factors influence image quality. For multi–detector row CT systems, a higher number of slices does not per se increase temporal resolution, but subsequent generations of CT, while increasing the number of detector rows, typically also provided faster rotation and hence higher temporal resolution. This schematic representation does not consider that by combining data from consecutive heartbeats, some multi–detector row CT systems allow reconstruction of images with shorter data acquisition windows than required for a 180° rotation

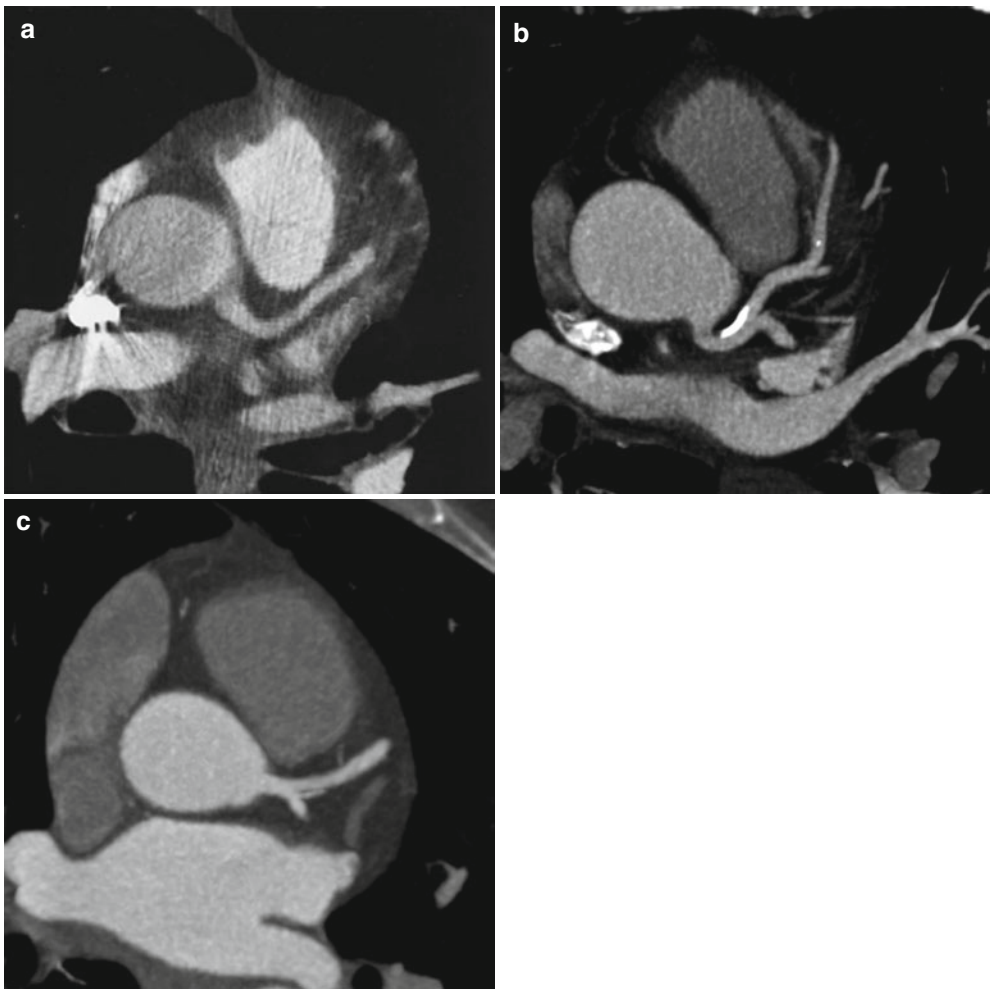

Fig. 1.7 Transaxial contrast-enhanced images obtained with various generations of multi–detector row CT (MDCT): (**a**) Four-slice CT with 4 × 1.0 mm collimation, 500 ms rotation time, and a temporal resolution of 250 ms. (**b**) 16-slice CT with 16 × 0.75 mm collimation, 375 ms rotation time, and a temporal resolution of 185 ms. (**c**) 64-slice CT with 64 × 0.6 mm collimation, 330 ms rotation time, and a temporal resolution of 165 ms

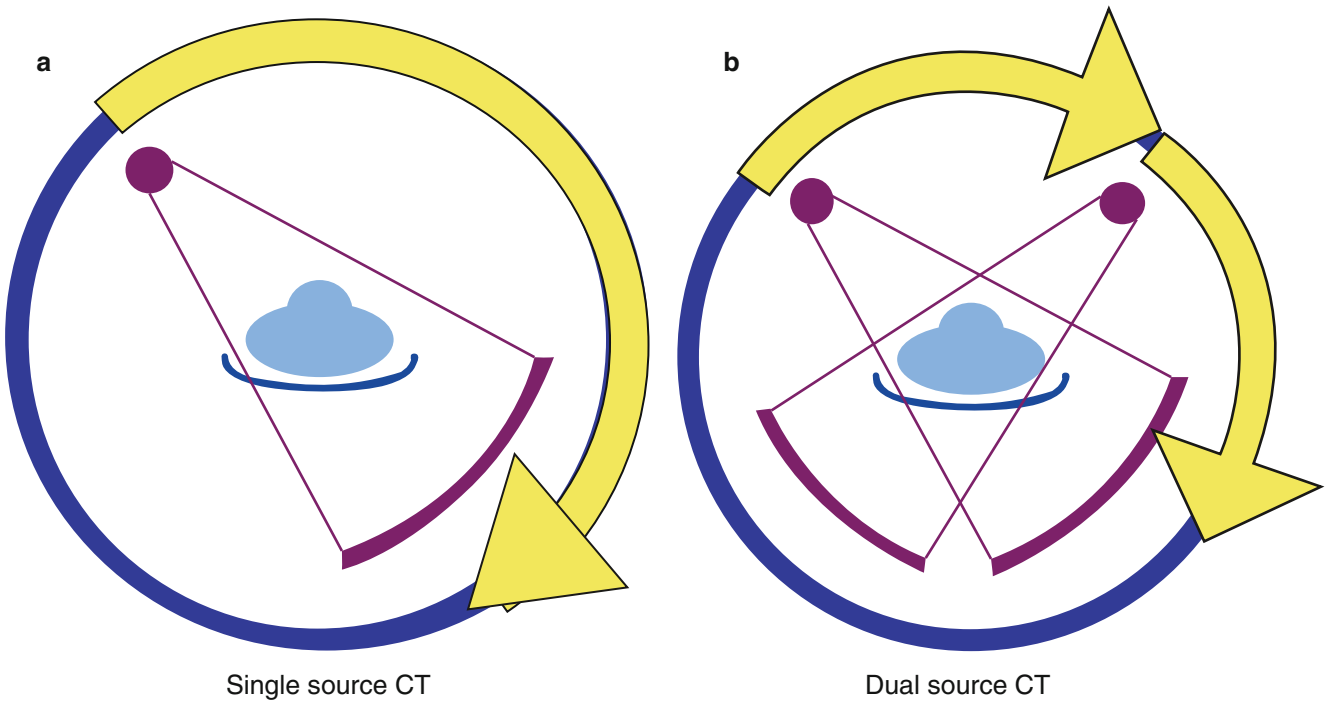

Fig. 1.8 Comparison of single-source and dual-source CT. Acquisition of X-ray data in projections over approximately 180° is required to reconstruct cross-sectional images. (**a**) In single-source CT, this requirement is achieved during approximately a half rotation of the X-ray tube and detector. (**b**) In dual-source CT, two sets of X-ray tube and detector are arranged at an angle of 90° and acquire data simultaneously. Hence, approximately a quarter rotation is sufficient to complete data acquisition, and temporal resolution is twice as high

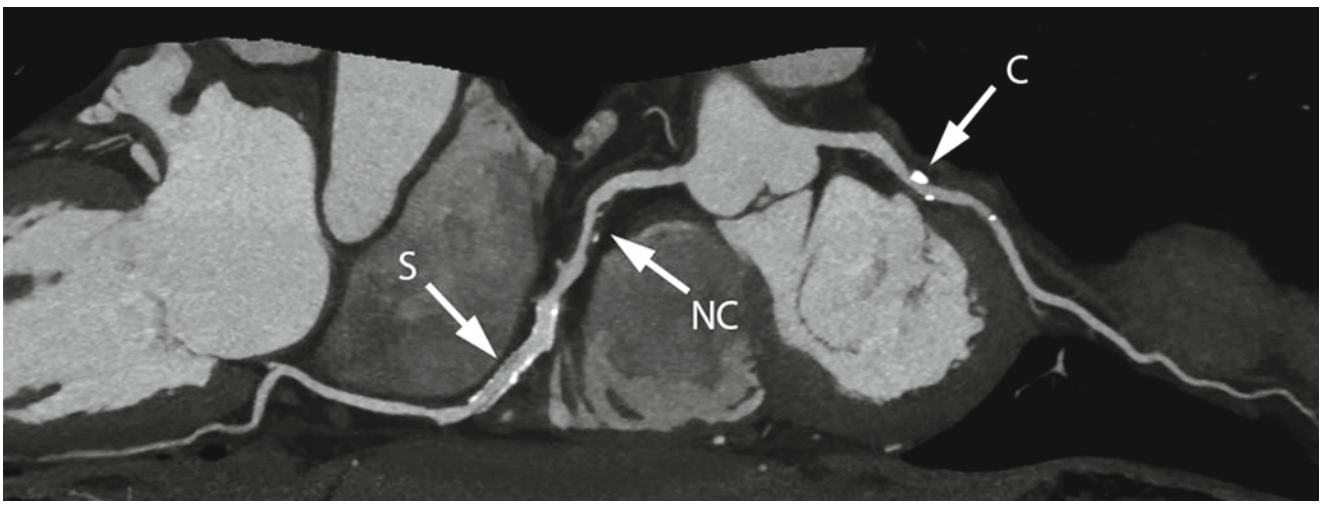

Fig. 1.9 Contemporary contrast-enhanced coronary CT angiography data set, in this case acquired with dual-source CT, 2 × 192 slice acquisition, 250 ms rotation time, and a temporal resolution of 66 ms. The image depicts a curved multiplanar reconstruction of the right and left circumflex coronary arteries, and shows examples of calcified plaque (C), noncalcified plaque (NC), and an implanted stent (S)

Fig. 1.10 Data acquisition modes in coronary CT angiography. (**a**) Retrospectively ECG-gated helical/spiral acquisition: During continuous table movement, the tube and detectors perform a helical/spiral path relative to the patient. X-ray data are continuously acquired with substantial oversampling (all levels of the heart are covered during several rotations); during the image reconstruction process, only data acquired at specific time instants of the cardiac cycle (e.g., mid diastole) are used. (**b**) Prospectively ECG-triggered axial acquisition: Data are acquired without table motion at a given level, and after completion of data acquisition, the table is moved to the next position. The X-ray tube is activated in synchronization with the patient's ECG ("ECG trigger"). The data acquisition window at each position can be kept very short so that radiation exposure is low. If the detector is wide enough (e.g., 320-slice CT), acquisition at only one table position can be sufficient. A complete data set can therefore be acquired within one single cardiac cycle. (**c**) Prospectively ECG-triggered high-pitch helical/spiral acquisition. This image acquisition uses very fast table speed so that a "pulled-open" spiral data set is acquired. At each level, just enough data are collected to reconstruct one image by combining detectors from the various detector rows. Subsequent images are reconstructed at slightly later time instants in the cardiac cycle

Modes of Data Acquisition and Radiation Exposure

Data acquisition in cardiac CT can follow various principles that have been developed over time as technology grew more sophisticated. Importantly, the mode of data acquisition has profound implications regarding radiation exposure. *Retrospectively ECG-gated acquisition* in "helical" mode (also called "spiral" mode) was the acquisition algorithm that was initially used for cardiac CT. Data are acquired during constant slow table motion with a relatively high amount of oversampling. It provides robust image quality and maximum flexibility to choose the cardiac phase during which images are reconstructed, including the ability to reconstruct dynamic data sets throughout the entire cardiac cycle, to assess ventricular function or valve motion. *Prospectively ECG-triggered axial acquisition* requires fast temporal resolution and relatively wide detectors because the images are acquired without table motion during the acquisition and with stepwise advancement of the patient table between consecutive heart beats. It is associated with substantially lower radiation exposure and image quality is high, especially in patients with stable and low heart rates. Less flexibility to reconstruct data at different time instants in the cardiac cycle, as well as greater susceptibility to artefacts caused by arrhythmia, can be downsides of this acquisition mode. In recent years, prospectively ECG-triggered axial acquisition has replaced retrospectively gated helical/spiral acquisition as the preferred acquisition mode in many experienced centers. Finally, *prospectively ECG-triggered high-pitch "helical" or "spiral" acquisition*, also referred to as "*Flash*" acquisition, is an imaging mode that combines aspects of the former two techniques, but it can be used only on selected dual-source CT systems and single-source CT systems with very wide detectors, and only in patients with low and truly regular heart rates. It can cover the volume of the heart within a very short time and maximizes the efficiency of radiation use, so that it is associated with very low radiation exposure (Fig. 1.10).

Next to the selected image acquisition mode, numerous other factors influence image quality and radiation exposure in cardiac CT. As coronary CT angiography (CTA) became a clinically useable imaging modality but hardware was not yet fully

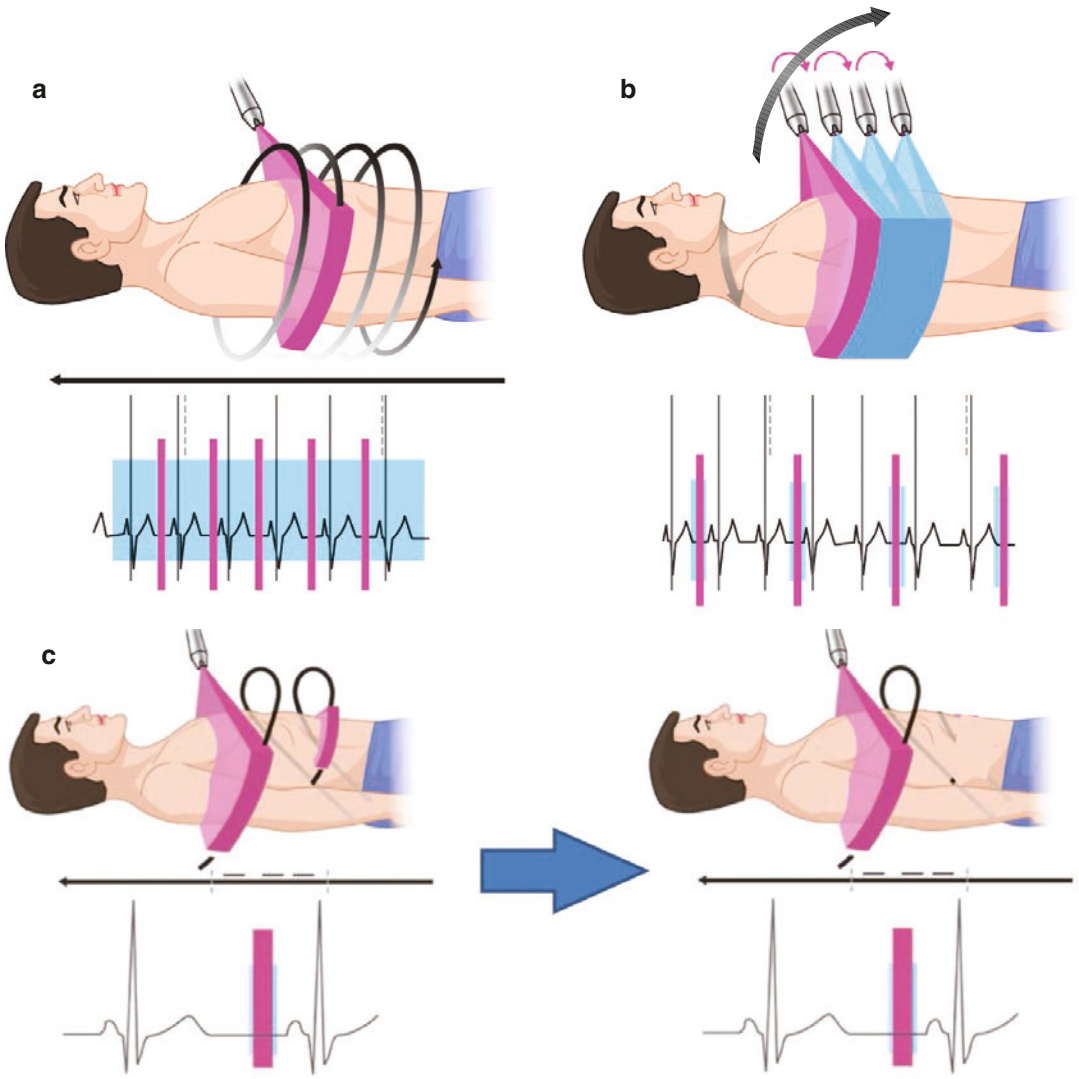

developed, radiation exposures were high. Subsequent improvements in scanner hardware, the development of the aforementioned image acquisition modes, further technical improvements, and physician education have led to a continued decrease in reported radiation exposures for coronary CTA. Currently, typical average effective doses range between 2 and 6 mSv [12, 13]. Effective doses below 1.0 mSv are well possible [14]. In very strictly selected patient cohorts, it has even been reported that doses of less than 0.5 mSv and even below 0.1 mSv can be achieved [15, 16]. Image quality at this extreme end of the spectrum is not robust enough for clinical application across a wide variety of patients, however (Fig. 1.11).

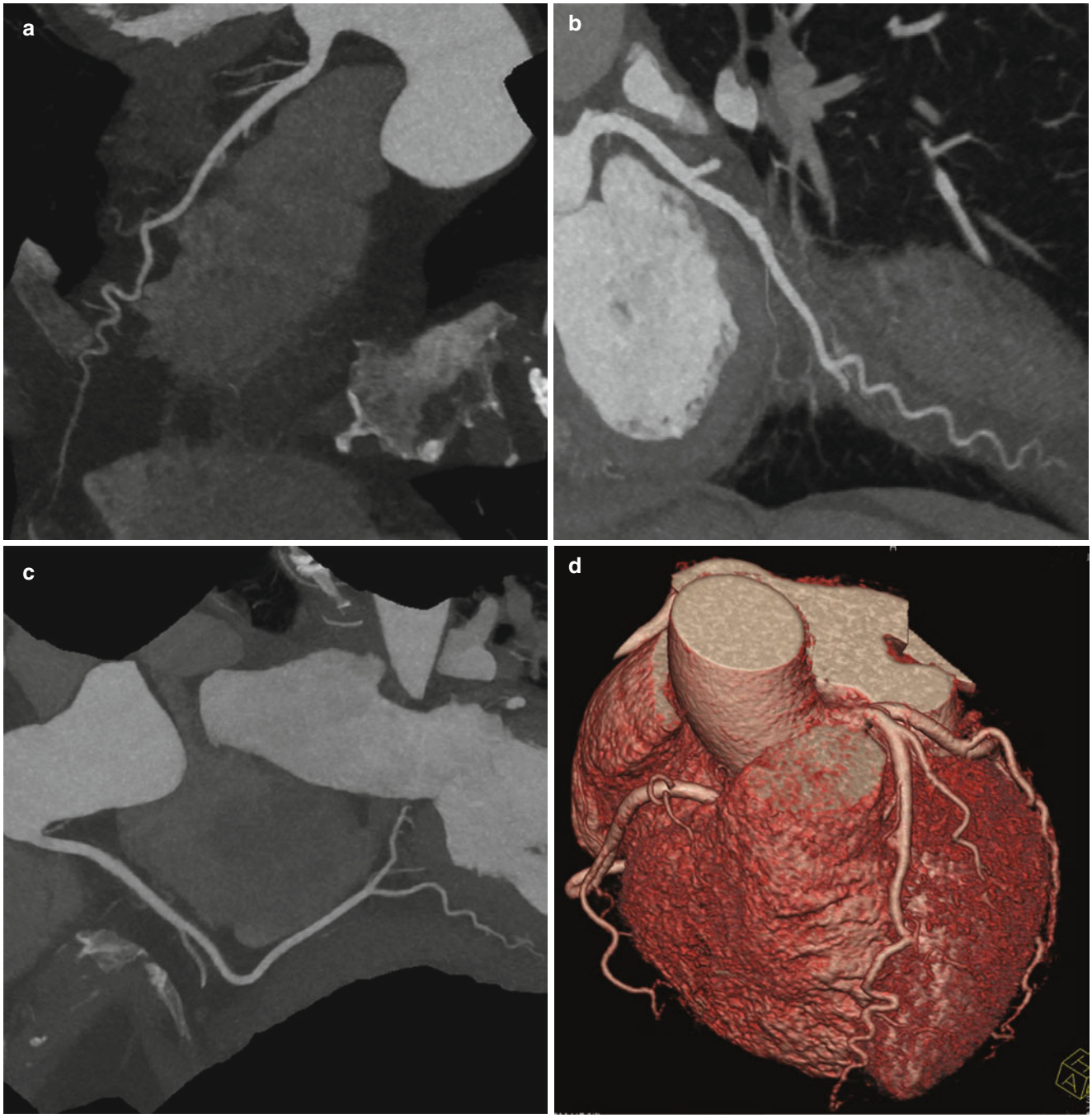

Fig. 1.11 Low-dose coronary CT angiography. By combining various methods to reduce radiation exposure, low-dose imaging is possible in coronary CT angiography. Here, the coronary arteries of a 56 years-old woman are depicted, based on a data set acquired with dual-source CT, using prospectively ECG-triggered high-pitch spiral acquisition at 70 kV tube voltage, with a dose-length product of 19.4 mGy/cm and an estimated effective dose of approximately 0.3 mSv. Image quality is high. Imaging at such dose levels is currently possible in only very selected patients with low body weight and low heart rates. (**a**) Curved multiplanar reconstruction of the left anterior descending coronary artery. (**b**) Curved multiplanar reconstruction of the left circumflex coronary artery. (**c**) Curved multiplanar reconstruction of the right coronary artery. (**d**) Three-dimensional reconstruction

Image Reconstruction and Post-processing

The technical development of cardiac CT has included not only hardware for data acquisition, but also the reconstruction algorithms that are used to generate images based on the acquired X-ray attenuation data. The conventional method to reconstruct images based on the acquired X-ray attenuation data is called "filtered back projection." Although this method does not make full use of the information in the X-ray data, it is computationally efficient and has therefore traditionally been used in order to keep image reconstruction time acceptable in clinical practice. "Iterative reconstruction" makes better use of the information in the X-ray attenuation data, but it requires substantially longer times for reconstruction than filtered back projection. Because modern computers provide increased processing power, iterative reconstruction methods can now be applied clinically and have been implemented on most CT systems that are used for cardiac imaging. Iterative reconstruction alters the visual impression of the reconstructed image data, but the substantial advantage is lower image noise. Hence, iterative reconstruction can be used either to improve image quality or, in combination with low-dose tube settings, to maintain an acceptable noise level in the images while substantially reducing radiation exposure [17] (Fig. 1.12).

Increasing computing power has affected not only image reconstruction based on X-ray attenuation data, but also the analysis of CT data sets. For example, fully automated algorithms can be used to evaluate coronary CTA data sets regarding the presence, volume, and type of atherosclerotic plaque [18]. Fluid dynamic modeling has been applied to simulate blood flow in the coronary arteries and permit

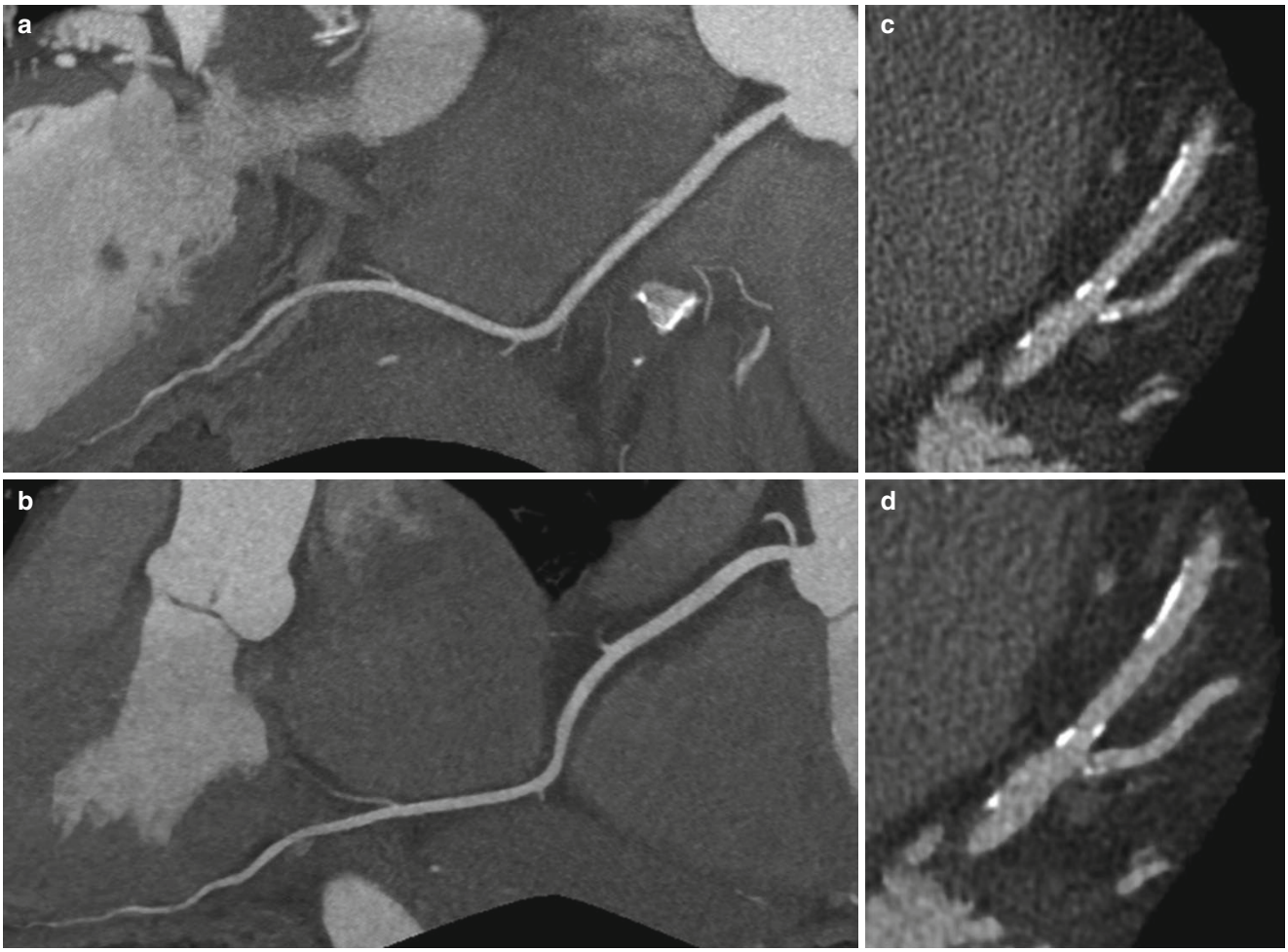

Fig. 1.12 Influence of iterative reconstruction on image quality. Identical raw data sets are reconstructed with traditional filtered back projection (**a**, **c**) and using more computationally elaborate iterative reconstruction (**b**, **d**), which has recently become available as a result of more sophisticated computing power. Noise in the image obtained with iterative reconstruction is considerably lower. Iterative reconstruction changes the image impression when compared with filtered back projection, but numerous authors have been able to show that the lower image noise allows the use of lower-radiation acquisition protocols while preserving diagnostic capability

virtual assessment of the fractional flow reserve (FFR-CT) [19]. It can be expected that software applications to evaluate cardiac CT data sets and to provide information beyond that visually assessable by a skilled interpreter will become even more widely available and clinically used in the future (Figs. 1.13 and 1.14).

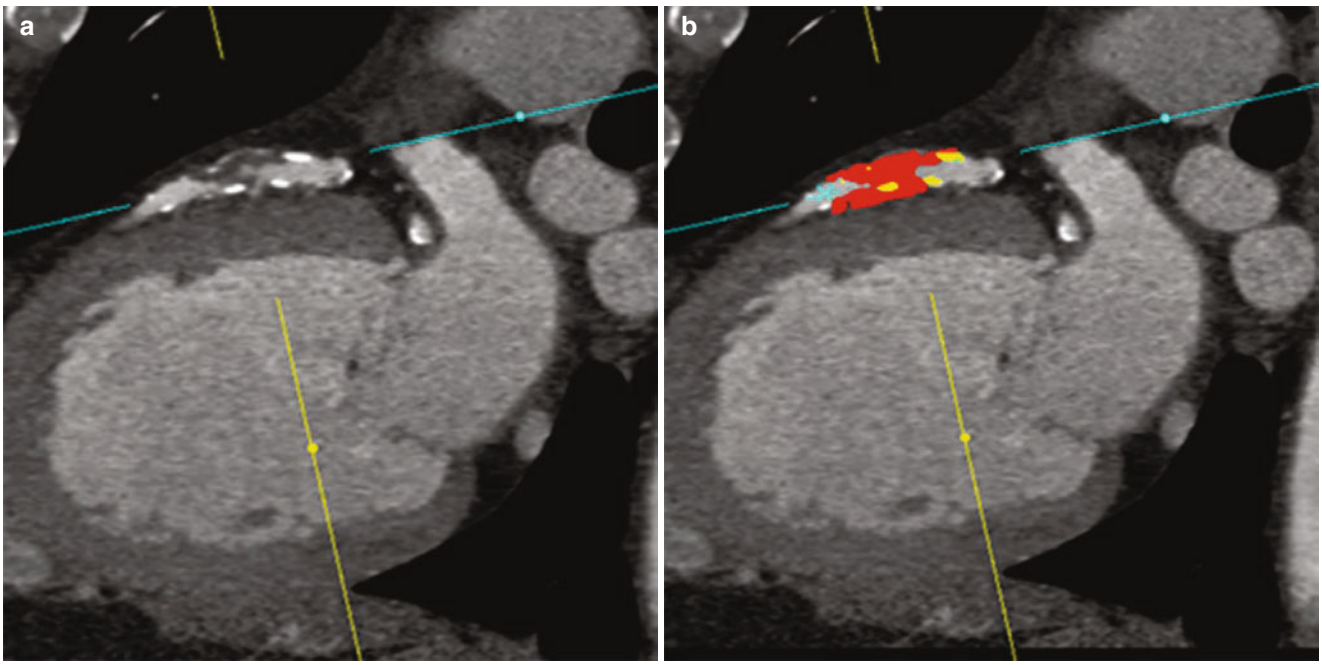

Fig. 1.13 Automated detection and characterization of coronary atherosclerotic plaque using specific software [18]. (**a**) Contrast-enhanced image of a proximal left anterior descending coronary artery showing complex plaque with positive remodeling. (**b**) The same image after automated identification of coronary atherosclerotic plaque (*red* = non-calcified plaque; *yellow* = calcified plaque). (*Images courtesy of* Dr. Damini Dey.)

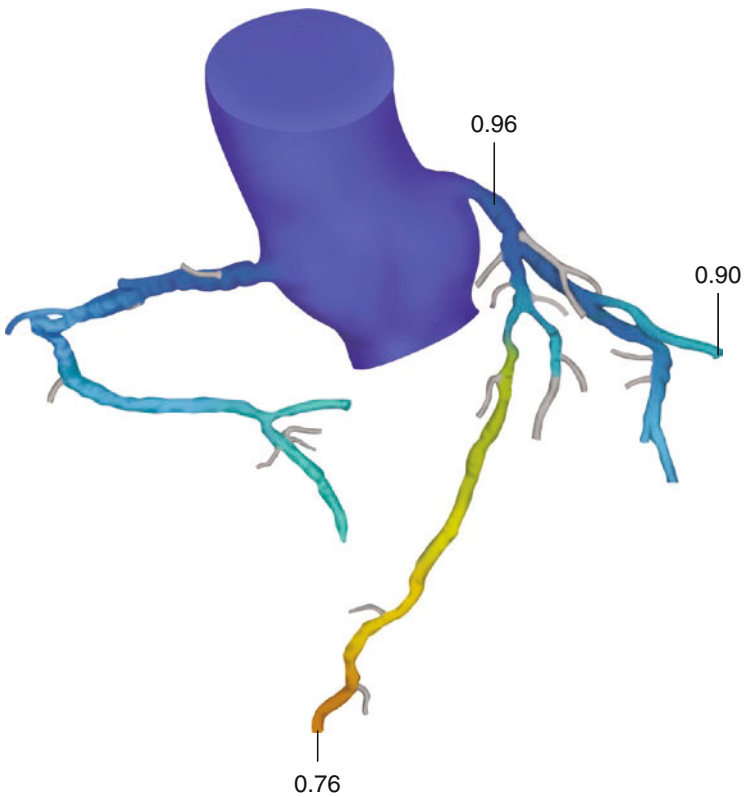

Fig. 1.14 Determination of virtual, CT-derived fractional flow reserve (FFR-CT). Based on the high-resolution anatomic data set obtained by coronary CT angiography, fluid dynamics modeling is used to simulate FFR (under the assumption of full microvascular dilatation) throughout the entire coronary tree [19]. According to published data, such simulated FFR-CT results correlate quite closely with invasively measured FFR values. In the "NXT Trial" [20], the sensitivity of FFR-CT to identify coronary lesions with an invasively measured FFR ≤ 0.80 was 86%, specificity was 79%, and overall accuracy was 81%

Noncoronary Applications of Cardiac CT

Since its development, the application of cardiac CT has focused on visualization of the coronary arteries—initially, on coronary calcium, and then almost entirely on contrast-enhanced coronary CT angiography. With the increasing robustness of cardiac CT, however, including its ease of applicability, coverage of large volumes, and low radiation exposure, and because of the growing need for high-resolution anatomic imaging in the context of complex interventions, noncoronary applications of cardiac CT play an increasingly important role in clinical practice. CT is used as an anatomic reference method for electrophysiologic interventions, to thoroughly assess patient characteristics before noncoronary interventions such as transcatheter aortic valve replacement (TAVR), and for the analysis of myocardial perfusion (Fig. 1.15).

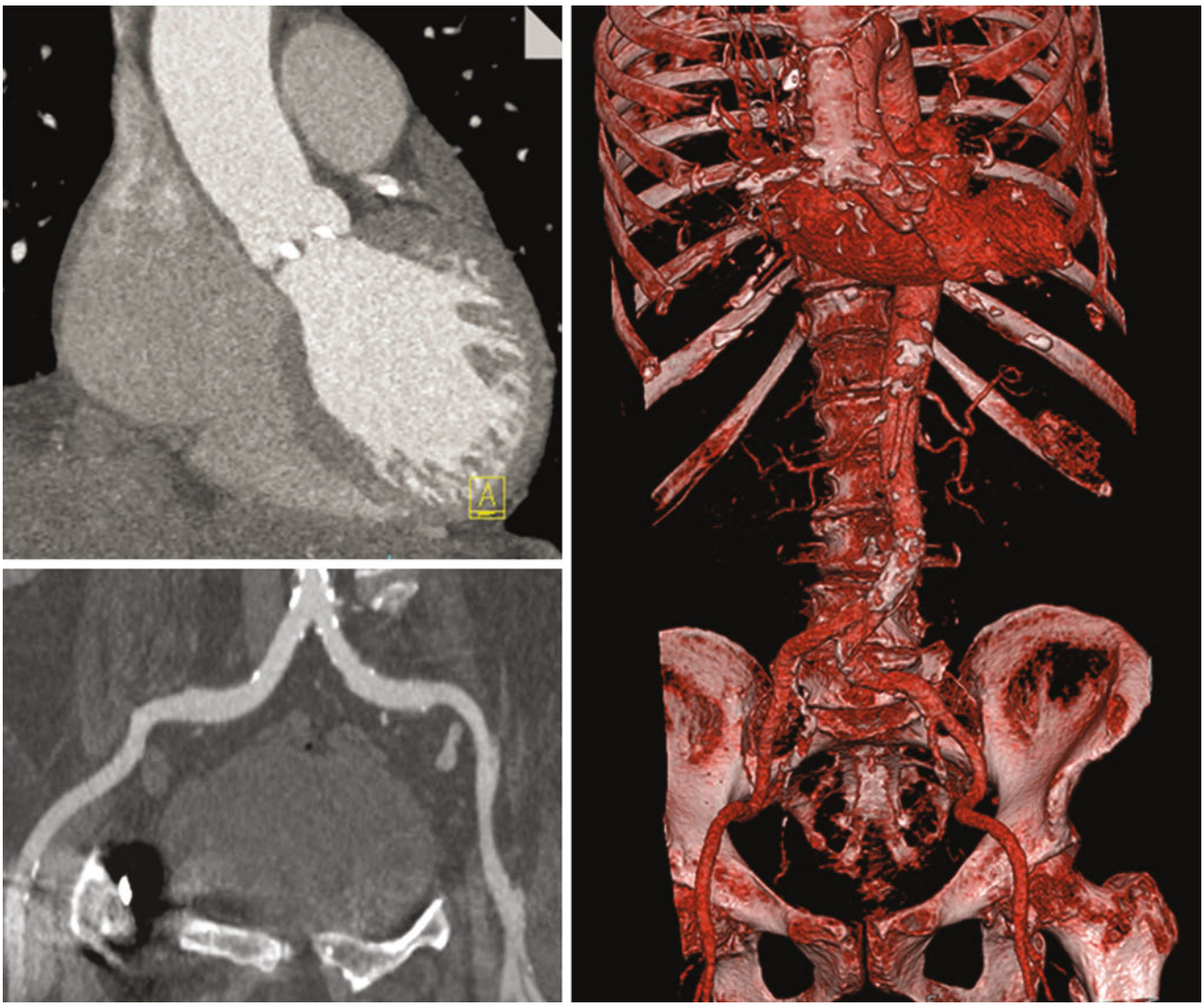

Fig. 1.15 Use of cardiac CT to assess a patient prior to transcatheter aortic valve replacement (TAVR). CT imaging is routinely used in candidates who undergo workup for potential TAVR. With high and isotropic spatial resolution and the ability to generate a large-volume data set within a short time, CT is well suited to support cardiac interventions by providing specific anatomic information. The 3D reconstructions show the scan range acquired with a single contrast bolus, in high-pitch acquisition mode within less than 1 s scan time. Out of this data set, information can be obtained regarding both aortic root anatomy (*top left*) and the anatomy of the pelvic and femoral access vessels (*bottom left*)

Future Developments

Future developments in cardiac CT will undoubtedly include a further evolution of technology with stronger X-ray tubes, faster gantry rotation, and more sophisticated detectors, such as photon count detectors that will provide increased resolution at lower noise. Along with the resulting increase in image quality, software applications for data reconstruction and analysis will expand the range of applications of cardiovascular CT, making coronary artery imaging even more robust and clinically applicable, and permitting new applications outside the coronary vessels.

References

1. Cormack AM. Reconstruction of densities from their projections, with applications in radiological physics. Phys Med Biol. 1973;18:195–207.
2. Hounsfield GN. Computerized transverse axial scanning (tomography) – part I. Description of the system. Br J Radiol. 1973;46:1016–22.
3. Kalender WA, Seissler W, Klotz E, Vock P. Spiral volumetric CT with single-breathhold technique, continuous transport, and continuous scanner rotation. Radiology. 1990;176:181–3.
4. Robb RA. The dynamic spatial reconstructor: An X-ray videofluoroscopic CT scanner for dynamic volume imaging of moving organs. IEEE Trans Med Imaging. 1982;1:22–33.
5. Lipton MJ, Higgins CB, Farmer D, Boyd DP. Cardiac imaging with a high-speed Cine-CT scanner: preliminary results. Radiology. 1984;152:579–82.
6. Agatston AS, Janowitz WR, Hildner FJ, Zusmer NR, Viamonte M Jr, Detrano R. Quantification of coronary artery calcium using ultrafast computed tomography. J Am Coll Cardiol. 1990;15:827–33.
7. Moshage WE, Achenbach S, Seese B, Bachmann K, Kirchgeorg M. Coronary artery stenoses: three-dimensional imaging with electrocardiographically triggered, contrast agent-enhanced, electron-beam CT. Radiology. 1995;196:707–14.
8. Schmermund A, Rensing BJ, Sheedy PF, Bell MR, Rumberger JA. Intravenous electron-beam computed tomographic coronary angiography for segmental analysis of coronary artery stenoses. J Am Coll Cardiol. 1998;31:1547–54.
9. Achenbach S, Moshage W, Ropers D, Nossen J, Daniel WG. Value of electron-beam computed tomography for the noninvasive detection of high-grade coronary-artery stenoses and occlusions. N Engl J Med. 1998;339:1964–71.
10. Achenbach S, Ulzheimer S, Baum U, Kachelriess M, Ropers D, Giesler T, et al. Noninvasive coronary angiography by retrospectively ECG-gated multislice spiral CT. Circulation. 2000;102:2823–8.
11. Flohr TG, McCollough CH, Bruder H, Petersilka M, Gruber K, Süss C, et al. First performance evaluation of a dual-source CT (DSCT) system. Eur Radiol. 2006;16:256–68. Erratum in Eur Radiol. 2006;16:1405.
12. Chinnaiyan KM, Boura JA, DePetris A, Gentry R, Abidov A, Share DA, Raff GL. Advanced Cardiovascular Imaging Consortium Coinvestigators. Progressive radiation dose reduction from coronary computed tomography angiography in a statewide collaborative quality improvement program: results from the advanced cardiovascular imaging consortium. Circ Cardiovasc Imaging. 2013;6:646–54.
13. Rochitte CE, George RT, Chen MY, Arbab-Zadeh A, Dewey M, Miller JM, et al. Computed tomography angiography and perfusion to assess coronary artery stenosis causing perfusion defects by single photon emission computed tomography: the CORE320 study. Eur Heart J. 2014;35:1120–30.
14. Achenbach S, Marwan M, Ropers D, Schepis T, Pflederer T, Anders K, et al. Coronary computed tomography angiography with a consistent dose below 1 mSv using prospectively electrocardiogram-triggered high-pitch spiral acquisition. Eur Heart J. 2010;31:340–6.
15. Schuhbaeck A, Achenbach S, Layritz C, Eisentopf J, Hecker F, Pflederer T, et al. Image quality of ultra-low radiation exposure coronary CT angiography with an effective dose <0.1 mSv using high-pitch spiral acquisition and raw data-based iterative reconstruction. Eur Radiol. 2013;23:597–606.
16. Hell MM, Bittner D, Schuhbaeck A, Muschiol G, Brand M, Lell M, et al. Prospectively ECG-triggered high-pitch coronary angiography with third-generation dual-source CT at 70 kVp tube voltage: Feasibility, image quality, radiation dose, and effect of iterative reconstruction. J Cardiovasc Comput Tomogr. 2014;8:418–25.
17. Naoum C, Blanke P, Leipsic J. Iterative reconstruction in cardiac CT. J Cardiovasc Comput Tomogr. 2015;9:255–63.
18. Dey D, Diaz Zamudio M, Schuhbaeck A, Juarez Orozco LE, Otaki Y, Gransar H, et al. Relationship between quantitative adverse plaque features from coronary computed tomography angiography and downstream impaired myocardial flow reserve by 13N-ammonia positron emission tomography: a pilot study. Circ Cardiovasc Imaging. 2015;8:e003255.
19. Min JK, Taylor CA, Achenbach S, Koo BK, Leipsic J, Nørgaard BL, et al. Noninvasive fractional flow reserve derived from coronary CT angiography: clinical data and scientific principles. JACC Cardiovasc Imaging. 2015;8:1209–22.
20. Nørgaard BL, Leipsic J, Gaur S, Seneviratne S, Ko BS, Ito H, NXT Trial Study Group, et al. Diagnostic performance of noninvasive fractional flow reserve derived from coronary computed tomography angiography in suspected coronary artery disease: the NXT trial (Analysis of Coronary Blood Flow Using CT Angiography: Next Steps). J Am Coll Cardiol. 2014;63:1145–55.

2 Preparation, Image Acquisition and Reconstruction, and Post-processing

Jamaluddin Moloo, Udo Hoffmann, and Harvey S. Hecht

Patient Selection and Preparation

There are no absolute contraindications to CT imaging. Table 2.1 lists the relative contraindications for the use of CT scans in cardiac imaging, and Table 2.2 outlines the steps in preparing a patient for the examination. The use of contrast agents contributes to the contraindications and preparatory steps. Traditionally, solid foods are discontinued 4 h before obtaining a contrast scan, to lower the risk of aspiration if a severe contrast reaction were to occur, but significant nausea and emesis occur infrequently with the use of modern contrast agents. Unless clinically contraindicated, liquids should be encouraged before the scan to ensure a patient is adequately hydrated to reduce the risk of contrast-induced nephropathy. Finally, patients with a contrast allergy require premedication to reduce the risk of a severe reaction.

Table 2.1 Patient selection: relative contraindications to cardiac CT

Relative contraindications
Pregnancy
Renal insufficiency (creatinine clearance <30 mL/min/1.73 m^2)
Radioactive iodine therapy (competitive binding with iodinated contrast)
Patient in an acute thyroid storm (can potentiate thyrotoxicosis)
Inability to perform breathhold ≥5 s

Table 2.2 Patient preparation

Prior to arrival
Consider holding caffeine 12 h before the scan if heart rate should be lower for the study
Consider beta-blocker administration to lower the heart rate (*e. g.*, metoprolol 50 mg PO 2 h prior to the study)
Discontinue phosphodiesterase inhibitors (if nitroglycerin will be utilized)
Consider holding nonsteroidal anti-inflammatory drugs (to limit the risk of contrast-induced nephropathy)
Hold glucophage the morning of the scan and for 48 h after
May continue other medications
No solid foods 4 h before the scan
May continue usual intake of liquids
Immediately before the scan (in holding area)
Obtain a brief history
Review indications
Screen for relative contraindications
Obtain IV access (ideally an 18 gauge in the R AC to allow injection of contrast at high flow rates of 5–7 mL/s)
Optimize heart rate with additional metoprolol IV if needed
Within the gantry
Heart should be centered within the gantry, to maximize spatial resolution
Appropriate placement of ECG leads
Provide nitroglycerin for coronary cases (0.4 mg SL or spray, to dilate coronaries and optimize coronary lumen visualization)
Practice breathhold and assess impact on heart rate
Optimize heart rate with additional metoprolol IV if needed

J. Moloo
Cardiac Vascular Center, University of Colorado, Denver, CO, USA
e-mail: jamaluddin.moloo@ucdenver.edu

U. Hoffmann (✉)
Department of Radiology, Massachusetts General Hospital, 165 Cambridge Street, Boston, MA 02114, USA
e-mail: uhoffmann@partners.org

H.S. Hecht
Department of Cardiology, Icahn School of Medicine at Mount Sinai, New York, NY, USA
e-mail: Harvey.Hecht@mountsinai.org

M.J. Budoff et al. (eds.), *Atlas of Cardiovascular Computed Tomography*, https://doi.org/10.1007/978-1-4471-7357-1_2

The Impact of Heart Rate

In photography, a moving object can be captured as a still image only if the shutter speed is sufficiently fast. The CT equivalent of shutter speed is gantry rotation time—that is, the time required for the radiograph tube and detector to rotate around the patient, thereby gathering the information needed to construct a single image. If the heart rate is higher than the temporal resolution of the CT scanner, motion artifact will obscure the CT image (Fig. 2.1). Newer generation CT scanners are able to obtain motion free images at significantly higher heart rates (70 bpm and higher). However, radiation dose generally increases as the heart rate increases given that the lowest dose imaging protocols are insufficient in such situations. The optimal heart rate for a given study is dependent on the indication for the study; for example, pulmonary vein imaging may be scanned at any heart rate while the ideal heart rate for coronary imaging is generally ≤60 bpm.

If the heart rate needs lowering, consider prescribing metoprolol 50 mg PO to be taken 2 h prior to the study (the peak serum concentration occurs approximately 1.5–2 h after oral administration). If additional B-blocker is needed after the patient arrives (ideally within a holding area), consider prescribing intravenous metoprolol, given in 5-mg increments up to 30 mg while monitoring clinical parameters (peak response of IV metoprolol occurs in approximately 20 min).

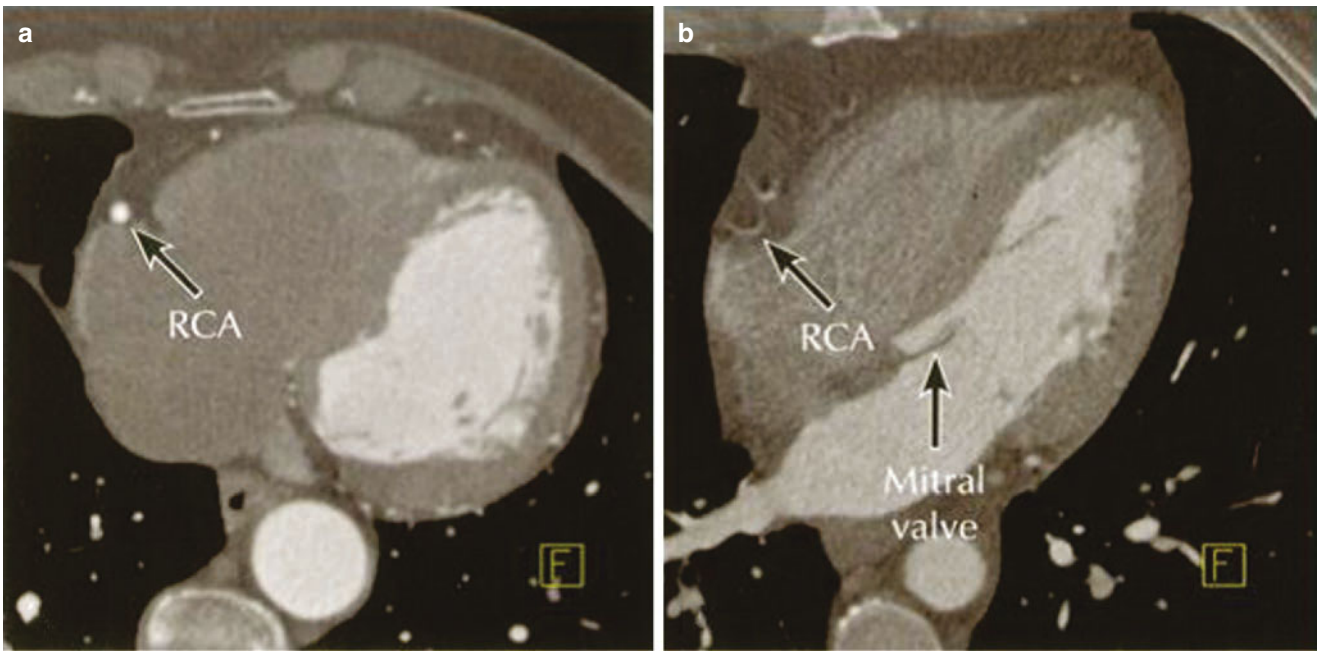

Fig. 2.1 Patient preparation: impact of heart rate. (**a**), Image obtained in a 74-year-old woman with a history of chest pain. The patient's mean heart rate at the time of image acquisition was 54 beats per minute and images were reconstructed in diastole at 65% of the R-R interval. The mid right coronary artery (RCA, *arrow*) shows sharp, distinct borders, and the lumen shows complete filling with contrast, without evidence of calcified or noncalcified plaque. (**b**), Image obtained in a 50-year-old man with a history of diabetes, dyslipidemia, and an equivocal nuclear stress test. The patient's mean heart rate at the time of image acquisition was 82 beats per minute and images were reconstructed in diastole at 65% of the R-R interval (mitral valve remains open; *arrow*). Motion artifact is substantial and obscures visualization of the mid RCA and the adjacent acute marginal branch (*arrow*). The streak pattern and central "hole" form a classic pattern of motion artifact

ECG Lead Placement

All cardiac studies are gated and hence require appropriate ECG lead placement. Artifact from external metallic devices, including ECG leads, may create streak artifact on CT images. To avoid artifact from ECG leads, the leads should be placed outside of the central field of view (Fig. 2.2). Once leads are in position, ensure that the scanner is appropriately sensing each R-wave. Occasionally, tall T-waves may be confused for the R-wave.

Breathhold Instructions

Motion artifact frequently limits one's ability to obtain CT images of diagnostic quality [1] (Fig. 2.3). Respiratory motion is an important source of motion artifact, and its impact is eliminated by acquiring all images during a breathhold, so that inability to perform an adequate breathhold is considered a relative contraindication to performing a cardiac CT. The duration of the breathhold varies depending on the scanning time. As the number of detectors has

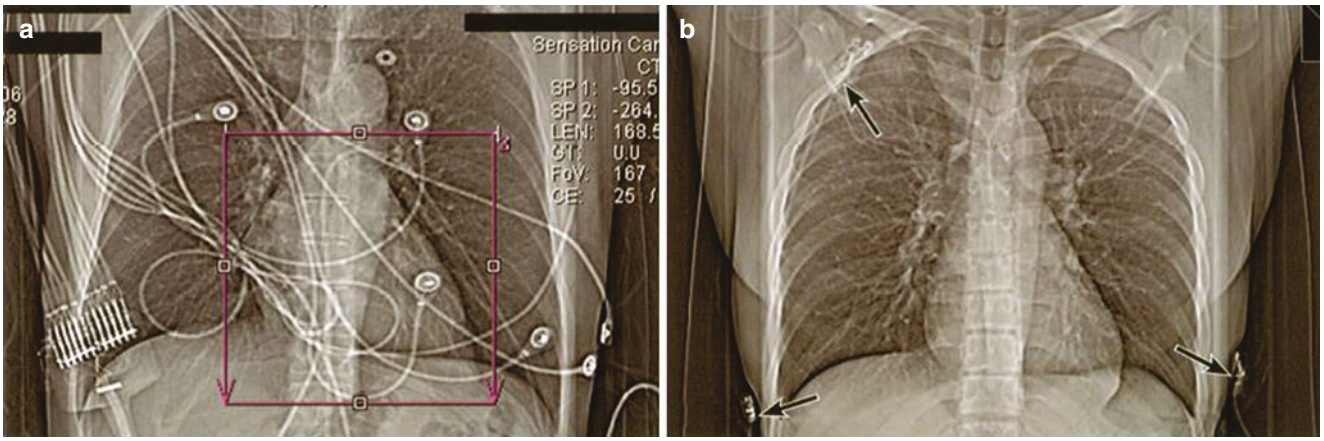

Fig. 2.2 Patient preparation: ECG lead placement. (**a**), A topogram of a patient whose ECG leads are incorrectly placed. The leads course over the chest wall and may create streak artifact. (**b**), Appropriate ECG lead placement (*arrows*) with the leads outside of the field of view. The "RA" ECG lead is placed over the right superior-lateral chest, and the "LL" ECG lead is placed in the left inferior-lateral chest; this pair generally provides an excellent rhythm strip, given its alignment along the cardiac electrical axis. A third "LA" ECG lead is then placed over the right inferior-lateral chest. The resultant rhythm strip should be reviewed to ensure that the R-wave is clearly visible and its amplitude is sufficient for ECG gating

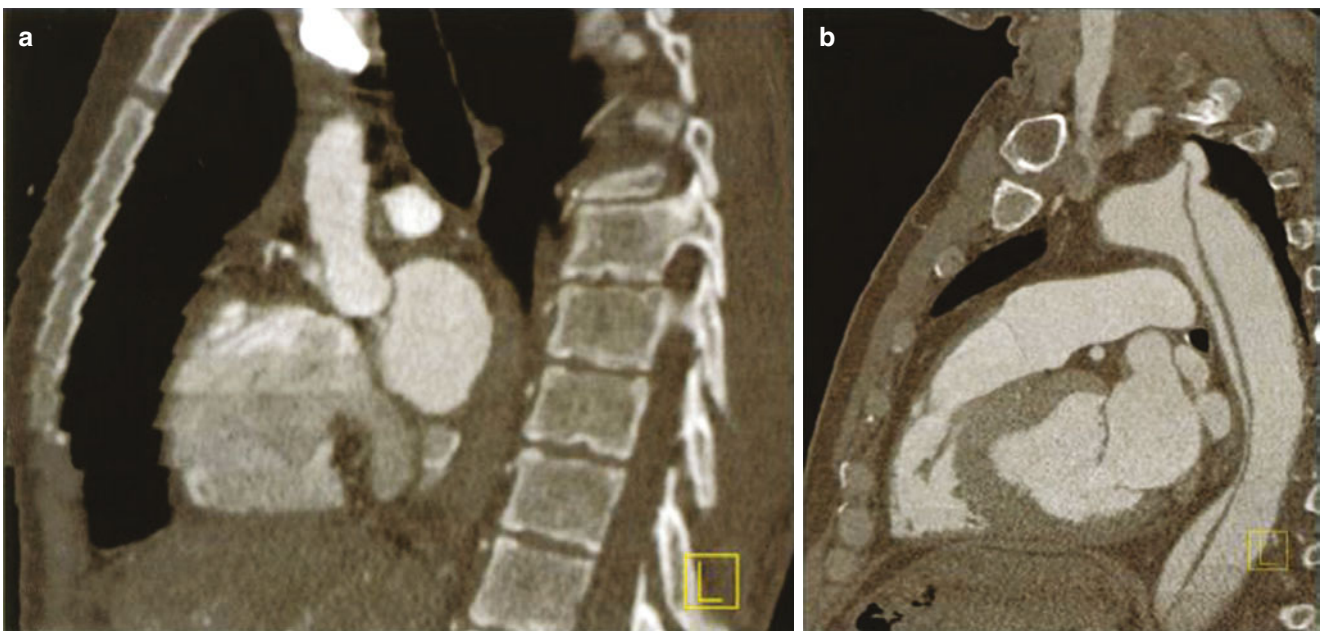

Fig. 2.3 Patient preparation: breathhold instructions. (**a**), A sagittal view of a patient who failed to appropriately hold her breath during image acquisition. The images were obtained in a cranio-caudal direction. Stair-step artifacts are visible over the sternum and the anterior myocardium, a consequence of exhaling during image acquisition. Respiratory artifact can be delineated from other forms of motion artifact most easily on such a sagittal view. (**b**), A sagittal view of a patient who was able to hold his breath appropriately; no evidence of motion is visible. This patient does have an aortic dissection extending from the left subclavian artery to the distal descending aorta

increased from 64 to 128 to 320, the area in the z-axis (cranio-caudal) covered by a single rotation of the gantry has increased, shortening the time required for image acquisition and for holding one's breath. With current scanners, a cardiac CT generally requires a 3–10-s breathhold. When obtaining a CT scan to assess coronaries, we tell the patient, "Take a breath in, breathe out, take a second breath in, and hold your breath." Thus, images are acquired at end inspiration. If the images are to be coregistered with a differing dataset, such as for pulmonary vein mapping and electrophysiologic studies, the CT images should be obtained at mid-expiration, allowing for improved coregistration. For pulmonary vein mapping, we tell the patient, "Take a breath in, breathe out, take a second breath in, breathe out, stop breathing." Of utmost importance is the need to practice the breathhold multiple times and ensure that the patient is able to comply.

Contrast Administration

Injection of an iodinated contrast agent allows one to enhance cardiac cavities and the coronary lumen so that they appear bright, in contrast to the surrounding tissues, myocardium, and epicardial fat. Appropriate delivery of the contrast agent is paramount to achieving diagnostic image quality (Table 2.3). To ensure adequate opacification of the coronary lumen (>300 HU), injection rates of 5–7 mL/s are used. Because the final concentration of contrast within the vessel lumen is dependent on the rate of injection and the patient's blood volume (which generally increases as patient size increases), we inject higher flow rates (6–7 mL/s) in larger or obese patients and in patients who have undergone coronary artery bypass grafting, to ensure maximal opacification of native vessels and the larger-gauge graft vessels. The total volume of contrast required is determined by the time required to complete image acquisition and rate of contrast injection. This ensures the presence of sufficient contrast within the distal coronary beds when the scanner reaches its most caudal location. Following contrast, saline is injected to ensure that the contrast bolus remains compact. Dual-head injectors should be used, typically with biphasic injection protocols. In a typical coronary study, 80 mL of contrast is injected at 5 mL/s and followed by 40 mL of saline at 5 mL/s. When right-sided visualization is required, such as for combined coronary and pulmonary embolus studies, a 50:50 mixture of contrast and saline replaces the saline flush.

Table 2.3 Use of contrast agents for cardiac CT

Contrast delivery rate
Coronary evaluation: 5–7 mL/s
CABG: May consider 6–7 mL/s
Contrast volume: Dependent on scanning time
Saline "chaser"
After test bolus: 20 mL NS
After full contrast: 40 mL NS

CABG Coronary artery bypass grafts, *NS* Normal saline

Image Acquisition and Reconstruction

Once a patient is adequately prepared and the contrast administration protocol has been established, the process of image acquisition can begin. The process of acquiring CT images can be broken down into three sequential steps. The first consists of obtaining a scout image of the chest, which is used to designate the anatomic region of interest. By narrowing the scanning field (cranialcaudal) to the region of interest, radiation exposure is minimized. To visualize the coronary lumen, image acquisition must be timed to coincide with the delivery of contrast to the coronary circulation. As such, the second step, contrast injection, is configured to ensure appropriate timing of scanning relative to the delivery of contrast. The final step involves selecting the appropriate parameters for cardiac CT image acquisition.

Figure 2.4 shows two topograms (similar to conventional chest radiographs) used to delineate the anatomic volume to be scanned as the first of the three image acquisition steps. Although protocols may differ by vendor, the topogram is always acquired as a low-energy scan. The tube voltage is set at 120 Kv and the amperage at 35 mAs.

A critical aspect of cardiac imaging is determining the contrast transit time. This allows one to ensure maximal contrast opacification of the coronary vessels during image acquisition, while minimizing radiation exposure. For coronaries, image acquisition should be initiated only after contrast reaches the coronaries from the patient's intravenous site (Figs. 2.5 and 2.6). Two methods, the test bolus method and the bolus trigger method, can be used to determine the time required for contrast to reach the coronaries. Both methods monitor contrast enhancement (in Hounsfield units) in the ascending aorta at the level of the carina, as a means of monitoring delivery of contrast to the coronaries. This information is utilized to calculate the total contrast transit time. The test bolus injection and breathing instructions are initiated at the same time (Fig. 2.5g). This approach requires that the rate of injection of the test bolus equals the rate utilized for the coronary evaluation sequence. The second approach to determining contrast transit time, the bolus tracking method, uses a series of low-dose axial scans (every 2 s) to track entry of contrast into the ascending aorta at the level of the carina. The coronary CT angiography imaging sequence is initiated when contrast enhancement reaches a predefined threshold, usually 100–110 HU. Both methods provide similar results in studies. An advantage of the test bolus method is it allows for a "trial run" in patients who may have difficulty following the instructions or those who have never had a contrast injection, as well as allowing one to gauge whether the heart rate is adequate for scanning. Disadvantages include the additional time required to perform the sequence and the additional 10 mL of contrast (Fig. 2.6).

As noted above, the final step in cardiac CT image acquisition involves selecting the appropriate imaging parameters. Among these is gantry rotation relative to movement of the scanner bed (Fig. 2.7). The CT gantry consists of a radiograph tube and a row of detectors opposite the tube. Photons traverse through the body from the tube to the detectors and are absorbed at differing rates by differing tissues; these differences are the basis on which CT images are developed. Given

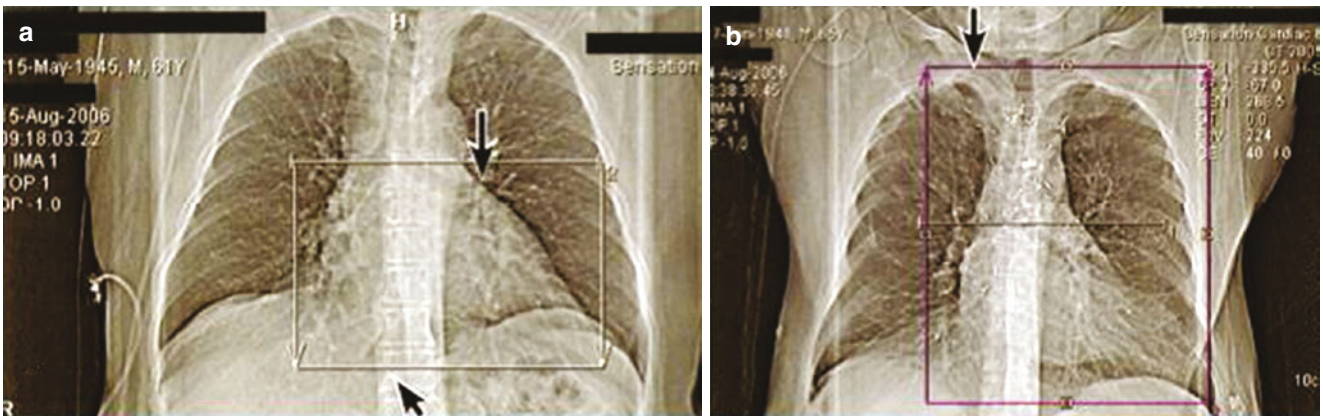

Fig. 2.4 (**a**), Topogram of a 61-year-old man with a history of chest pain and dyspnea on exertion. Evaluation of this patient requires imaging of the coronaries from their origin to the inferior aspect of the heart. As such, markers were set (*arrows*) to initiate scanning at the carina and end where the inferior aspect of the heart is projected to lie. Frequently the inferior aspect of the myocardium must be estimated, because the heart silhouette is incompletely visualized below the dome of the diaphragm. The scanning range should be extended an extra 1–2 cm in case the patient's inspiratory breathhold increases, secondarily shifting the heart caudally during coronary image acquisition. (**b**), Topogram of a 65-year-old man with prior coronary artery bypass grafting (CABG), with a recent nondiagnostic nuclear stress test. The exercise stress test was considered nondiagnostic because of a failure to achieve an adequate heart rate. Markers were set to initiate imaging at the clavicles to include the origins of internal mammary grafts (*arrow*). The breathhold duration is determined by and equal to the time required to acquire images. Heart coverage is possible within a single breathhold of 13 s with 32-slice CT, and 5–10 s with 64-slice CT. Imaging of patients who have undergone CABG requires breathholds approximately 30% longer in duration (if the internal mammary artery is imaged at its origin)

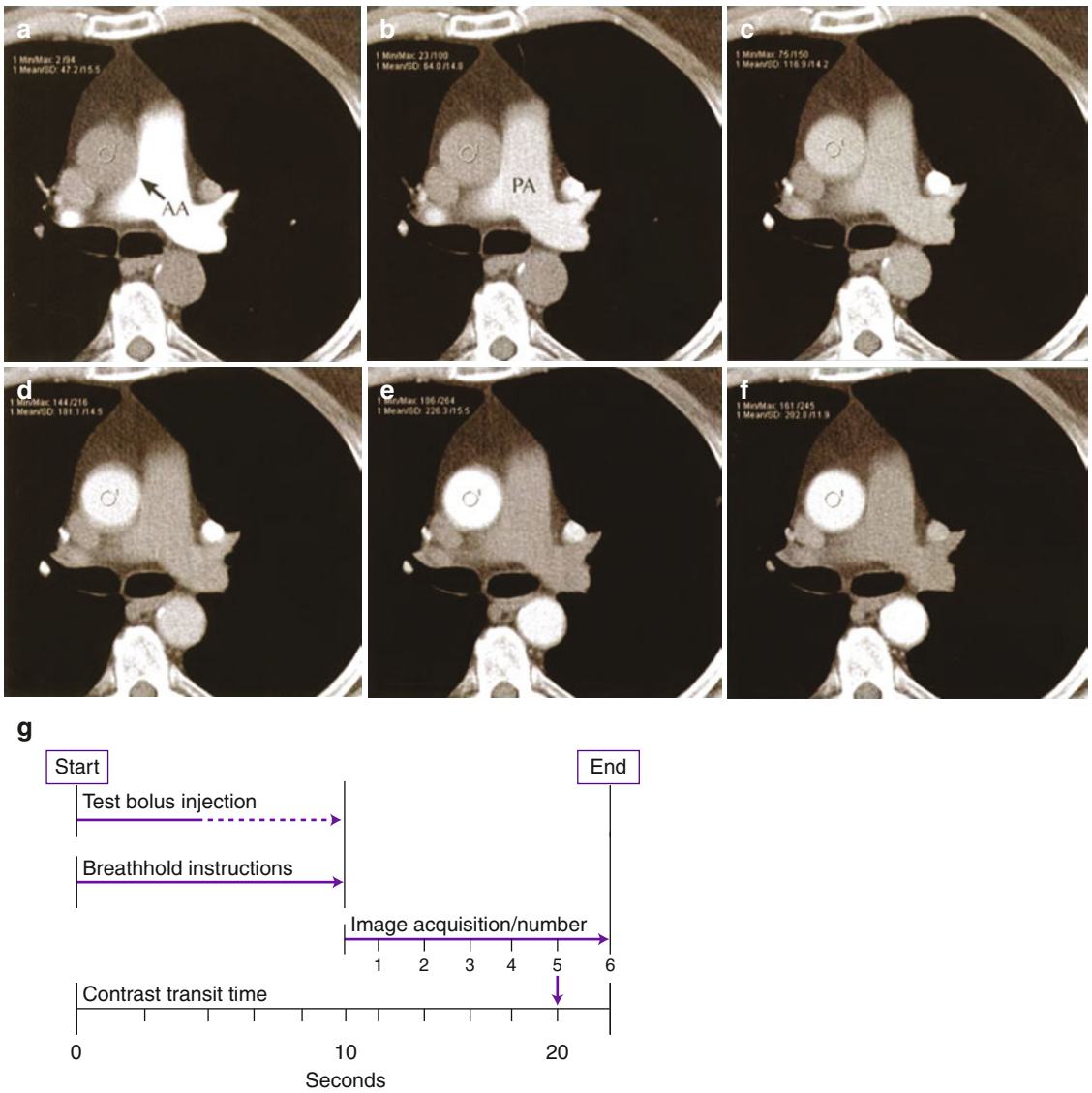

Fig. 2.5 Image acquisition: determining contrast transit time. (**a**–**f**), The test bolus method monitors contrast enhancement in the ascending aorta (AA; *arrow*) at the level of the carina, as a means of monitoring delivery of contrast to the coronaries. In the test bolus, 10 mL of iodinated contrast is injected at 5–7 mL/s, followed by a saline chaser. These six sequential, ungated axial images were obtained at 2-s intervals after injection; the flow of contrast is monitored as it enters the pulmonary outflow tract (**a**) and subsequently returns to the left side with maximal opacification in the aorta (Ao) occurring in image (**e**). This information is utilized to calculate the total contrast transit time. (**g**), Diagram showing that the test bolus injection and the breathing instructions are initiated at the same time point. Breathing instructions are constructed to extend for a total of 10 s; at completion of the breathing instructions, the patient will have initiated the breathhold, allowing one to initiate imaging. Knowing that peak enhancement was achieved on image (**e**) and given that each image was obtained at 2-s intervals results in a contrast transit time of 20 s (10 s for the breathhold plus 10 s, given that peak enhancement was achieved on image #5). Thus, for coronary CTA image acquisition, scanning should be delayed for 20 s after initiating injection of contrast in this patient. *PA* pulmonary artery

that the photons traverse through the patient, images can be reconstructed using data from half a rotation of the gantry around the patient. Hence, the standard mode by which CT images are reconstructed is a "half-scan" reconstruction algorithm. As the gantry rotates around the patient, the scanner bed moves forward, producing a spiral path relative to the patient, hence the term *spiral* or *helical* CT. More recently, axial or "step and shoot" acquisitions are employed in prospectively gated studies. In axial mode, the scanner bed remains in place while the gantry rotates around the patient then moves in a step wise fashion as each additional set of axial images is acquired.

Another important parameter is pitch. As the gantry rotates around the patient, the scanner bed advances. If the bed advances more quickly relative to the time it takes for the gantry to revolve around the patient and acquire a set of axial

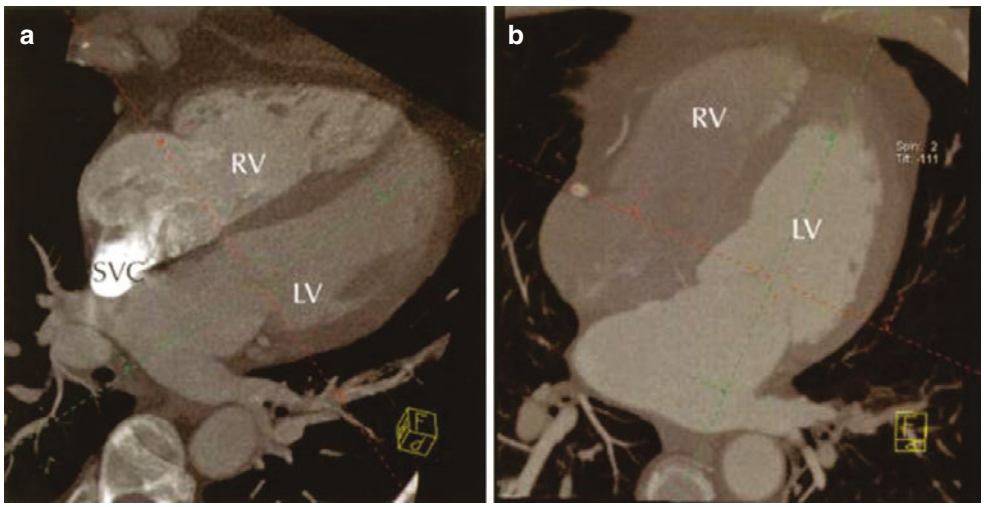

Fig. 2.6 Image acquisition: contrast timing. (**a**), In this example of image acquisition occurring too early, contrast is still visible entering the superior vena cava (SVC), and enhancement is greater within the right ventricle (RV) than in the left ventricle (LV). Coronary vessel assessment is usually severely limited in such cases. (**b**), In this example of optimal timing of contrast injection, contrast within the right ventricle is minimal, and the greatest contrast is seen within the left ventricle and the coronaries

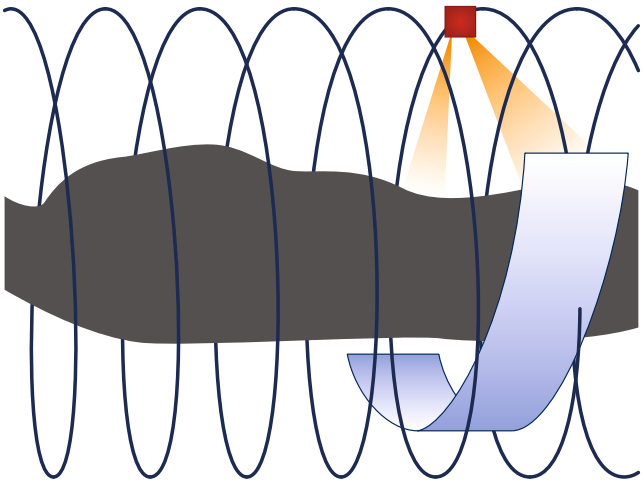

Fig. 2.7 Image acquisition: gantry rotation. The standard mode by which CT images are reconstructed is a "half-scan" reconstruction algorithm. As the gantry rotates around the patient, the scanner bed moves forward, producing a spiral path relative to the patient

slices, gaps are created in the data/image set, whereas if the bed advances slowly, data overlap (Fig. 2.8). Although the pitch used during acquisition differs across differing vendors, most utilize a pitch of approximately 0.2–0.3. The advantage of using a pitch less than one and acquiring overlapping data is that it allows greater flexibility when reconstructing images. For example, if a premature ventricular contraction occurs during scanning one is able to "ignore" data from the PVC and reconstruct the image using data from the next heart-beat. Overlap also decreases the amount of artifact created as the gantry rotates around the patient, and it improves the signal-to-noise ratio of the images. The drawback to utilizing a lower pitch is its higher radiation dose. Thus, protocols aim for a compromise between image quality and radiation exposure. Fast-pitch scanners have been introduced to dramatically shorten the acquisition times and radiation exposure, but these are most suitable for low heart rates.

Scanners with 64 or 128 detectors are unable to obtain cardiac images in a single rotation, which can be done routinely using 320-detector scanners. Because the heart is constantly oscillating between systole and diastole, images must be constructed at a given phase of the R-R interval to minimize motion artifact. *Retrospective acquisition* allows one to obtain images throughout the entire cardiac cycle and construct cine images, which are used to evaluate wall motion, ejection fraction, and valvular function. All cardiac CT images are ECG-gated, and retrospective studies are typically reconstructed at 10% intervals. Figure 2.9 illustrates several ECG rhythm strips with the associated CT tube current, the final parameter to be selected along with KVp. To lower radiation exposure [2], one can turn on tube modulation and lower the tube current during phases not being used for image reconstruction. Images produced when the tube current is lowered are of lower quality, but they are of sufficient quality to evaluate noncoronary structures. The radiation dose reduction depends on the heart rate; it varies between 30 and 50%, but the dose is lowered more in patients with lower heart rates. Dose modulation should be utilized in all retrospective acquisitions unless optimal images are needed throughout the entire cardiac cycle (i.e.: when evaluating an atrial septal defect or a paravalvular leak).

Although specifications differ by vendor, typical image acquisition parameters include a kilovoltage peak (kVp) of 120 kVp for larger patients, 100 kVp for intermediate sizes, and 80 kVp for small patients; exposure time in milliamp seconds (mAs), ranging from 600 to 900 mAs; slice thickness of

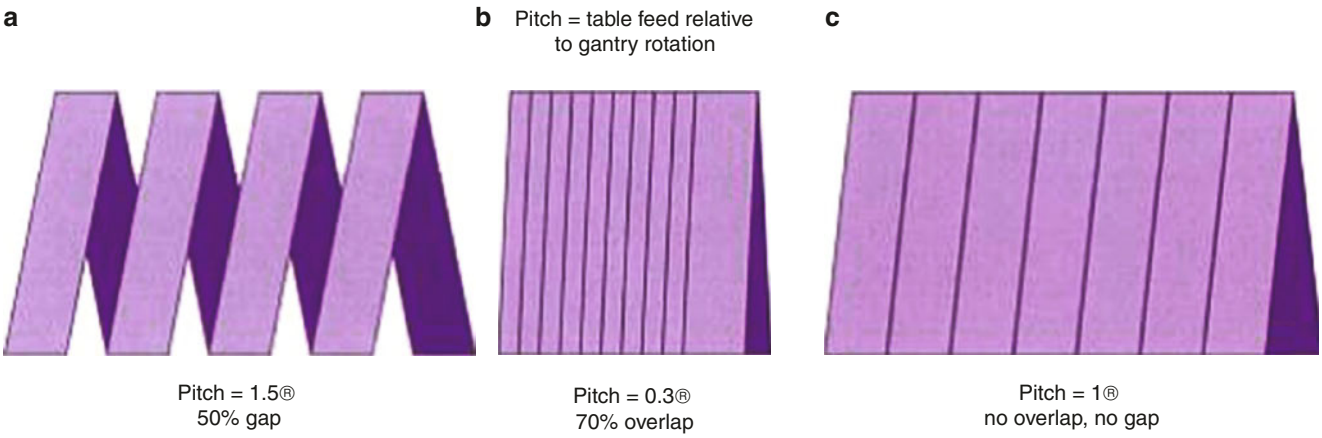

Fig. 2.8 Image acquisition: pitch. (**a**), A pitch of 1.5 is set, providing a gap of 50%. (**b**), A pitch of 0.3 produces 70% overlap. (**c**), A pitch of 1, with no overlap. (*Courtesy of* Dr. S. Abbara.)

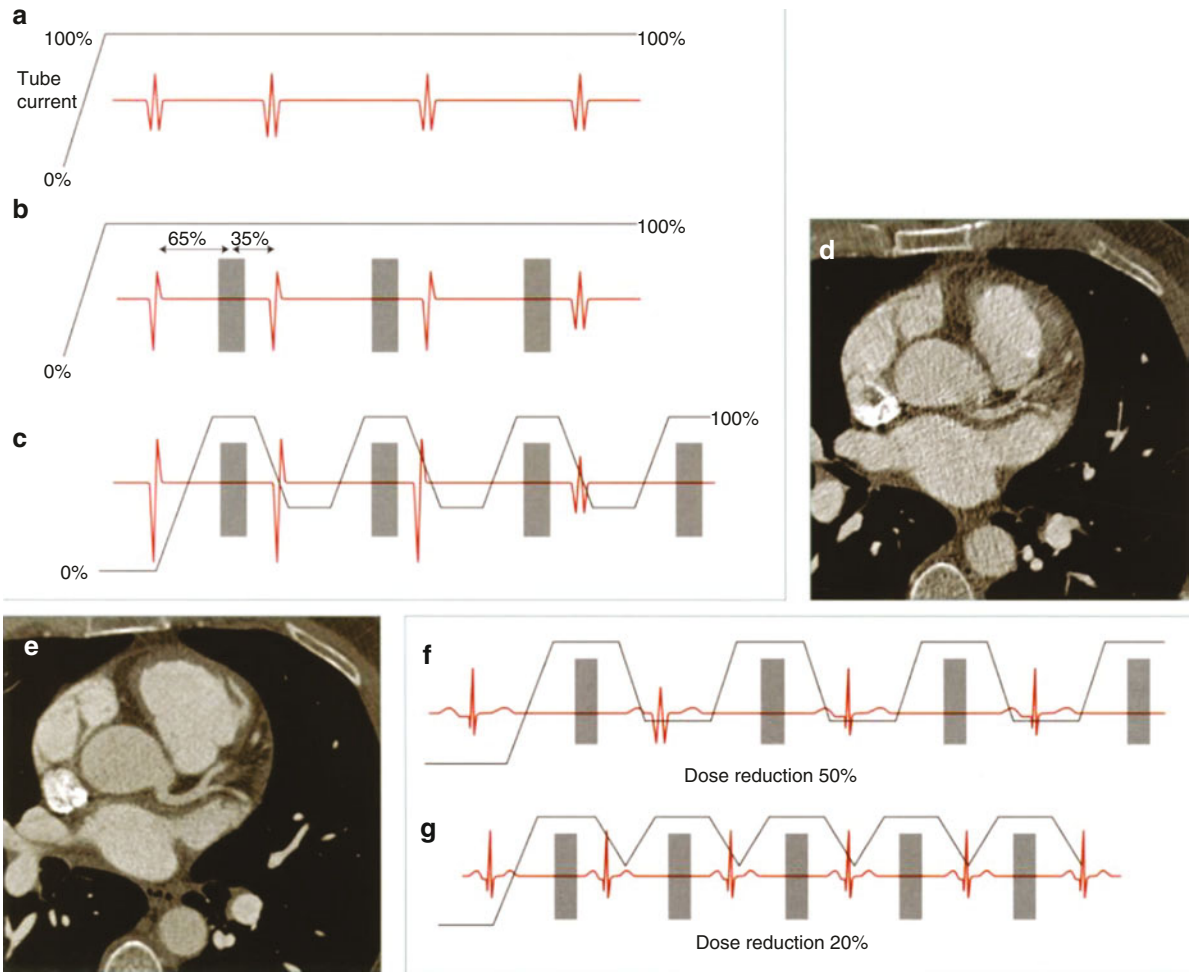

Fig. 2.9 Image acquisition and reconstruction. (**a**), An ECG rhythm strip and the associated CT tube current (a). In this case of retrospective acquisition, the tube current is turned to 100% at the start of image acquisition and remains so till completion of the study. For this patient in normal sinus rhythm, image reconstruction is at 65% of the R-R interval, and the tube current is at 100% (**b**). Tube modulation (**c**) is used to lower the tube current during phases not being used for image reconstruction. Image produced when the tube current is lowered; the image quality is reduced (**d**). Image produced when the tube current is 100% (**e**). Comparison of these strips shows that the radiation dose is lowered to a greater extent in patients with lower heart rates (**f** and **g**). (Parts A–C, F, and G *adapted from* Dr. S. Abbara.)

0.5–0.625 mm; and a pitch of 0.2–0.3. The scanning direction is generally craniocaudal. In obese individuals (>200 pounds), the mAs may be increased to reduce image noise. Alternatively, slice thickness may be increased to 1 mm, which improves the signal-to-noise ratio at the expense of lower spatial resolution.

With *prospective* (axial or step and shoot) *acquisition*, current is applied only during a specified phase, usually 75% of the R-R interval, or slightly longer (padding), resulting in a dramatic reduction in radiation exposure, proportional to the number of acquired phases. The 40% phase may be used at higher heart rates. Prospective acquisition is preferred to retrospective imaging given lower radiation doses. Retrospective imaging should be reserved for specific cases such as irregular or rapid heart rates, or for the evaluation of valvular function.

Standard reconstruction algorithms employ filtered back projection, but more recently, *iterative reconstruction* (IR) has become available on all scanners and yields a significant improvement in signal-to-noise ratio with smoother images. This improvement facilitates radiation dose reduction proportional to the iterative reconstruction level, sometimes exceeding 50%. Iterative model-based reconstruction (IMBR) provides even greater improvement in signal-to-noise ratio and radiation dose reduction. Such iterative reconstruction algorithms are becoming the standard of care.

Post-processing

Once the axial dataset has been obtained, the post-processing phase begins. The primary objective of the post-processing phase is to reconstruct the axial data and construct a specific set of images allowing one to evaluate the coronaries, cardiac function (data is not available in prospective studies), and extracardiac anatomy. A systematic approach simplifies this process (Fig. 2.10). For coronary evaluation, the steps include (1) Review of the ECG for ectopy or arrhythmias, which may impact the quality of images constructed. (2) Selection of the optimal phase for image reconstruction, to avoid motion artifact. (3) Selection of the kernel and reconstruction parameters; this choice will be influenced by the presence of stents and other patient factors. (4) Review of the source (axial) dataset. (5) Evaluation of potential stenoses in the true short axis using maximum intensity projection (MIP) images and multiplanar reformats (MPR). (6) Confirmation of stenoses in a second phase. To evaluate cardiac function, one should construct a dataset that captures images across the entire cardiac cycle and evaluate cine images. A dataset including the full field of view is constructed to evaluate extracardiac anatomy.

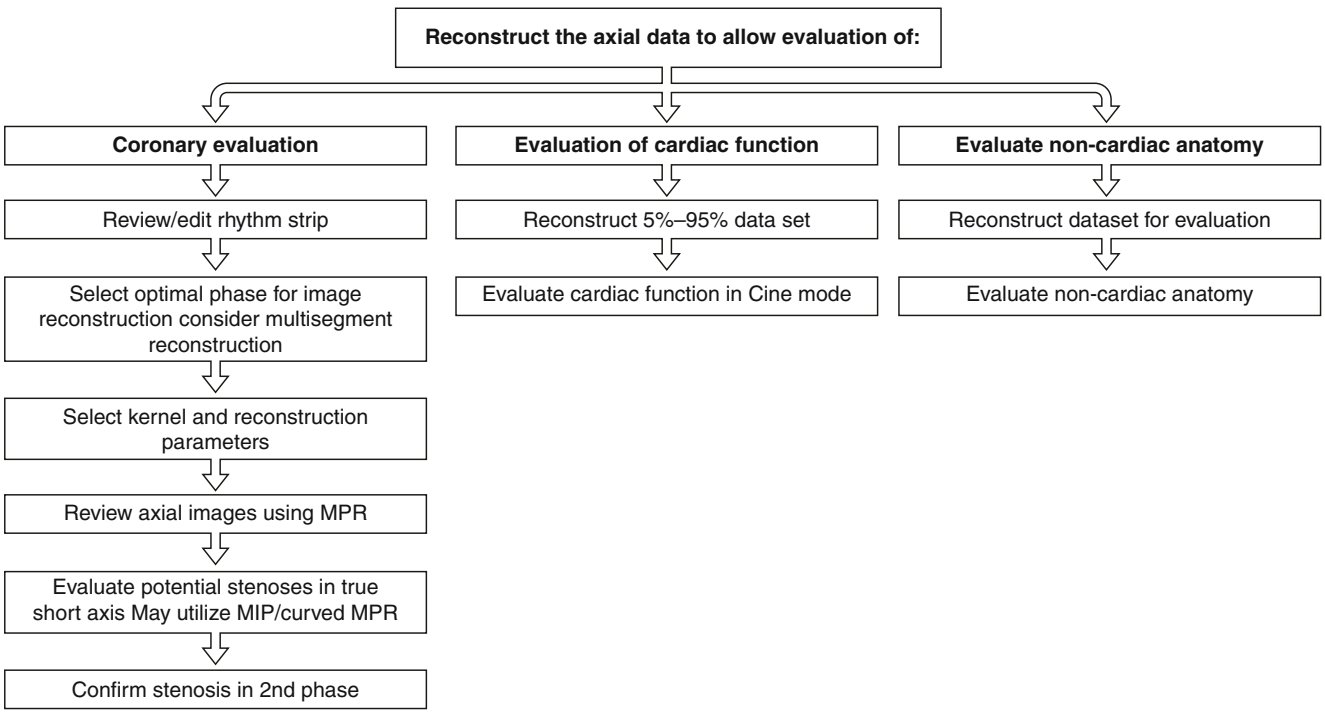

Fig. 2.10 Post-processing: objectives. A systematic approach to the evaluation of the coronaries, cardiac function, and noncardiac anatomy. *MIP* maximum intensity projection, *MPR* multiplanar reformats